Elsevier Editorial System(tm) for Geomorphology

Manuscript Draft

Manuscript Number: GEOMOR-564R1

Title: Using geomorphic and biological indicators of coastal uplift for the evaluation of paleoseismicity and Holocene uplift rate at the footwall of a normal fault (western Corinth Gulf, Greece)

Article Type: Research Paper

Section/Category:

Keywords: Holocene shorelines; Coastal fault zone; Coastal uplift; Paleoseismology; Shore platforms; Gulf of Corinth

Corresponding Author: Dr Nikolaos Palyvos, Ph.D

Corresponding Author's Institution:

First Author: Nikolaos Palyvos

Order of Authors: Nikolaos Palyvos; Francis Lemeille; Denis Sorel; Daniela Pantosti; Kosmas Pavlopoulos; Nikolaos Palyvos, PhD; Francis Lemeille; Denis Sorel; Daniela Pantosti; Kosmas Pavlopoulos

Manuscript Region of Origin:

Abstract: The westernmost part of the Gulf of Corinth (Greece) is an area of very fast extension (~15 mm/yr according to geodetic measurements) and active normal faulting, accompanied by intense coastal uplift and high seismicity. This study presents geomorphic and biological evidence of Holocene coastal uplift at the western extremity of the Gulf, where such evidence was previously unknown. Narrow shore platforms (benches) and rare notches occur mainly on Holocene littoral conglomerates of uplifting small fan deltas. They are perhaps the only primary paleoseismic evidence likely to provide information on earthquake recurrence at coastal faults in the specific part of the Rift system, whereas dated marine fauna can provide constraints on average Holocene coastal uplift rate.

The types of geomorphic and biological evidence identified are not ideal, and there are limitations and pitfalls involved in their evaluation. In a first approach, 5 uplifted paleoshorelines may be indentified, at 0.4-0.7, 1.0-1.3, 1.4-1.7, 2.0-2.3 and 2.8-3.4 m a.m.s.l. They probably formed after 1728 or 2250 Cal. B.P. (depending on the marine reservoir correction used in the calibration of measured radiocarbon ages). A most conservative estimate for the average coastal uplift rate during the Late Holocene is 1.6 or 1.9 mm/yr minimum (with different amounts of reservoir correction). Part of the obtained radiocarbon ages of Lithophaga sp. allows for much higher Holocene uplift rates, of the order of 3-4 mm/yr, which cannot be discarded given that similar figures exist in the bibliography on Holocene and Pleistocene uplift at neighbouring areas. They should best be cross-checked by further studies though.

That the identified paleoshoreline record corresponds to episodes of coastal uplift only, cannot be demonstrated beyond all doubt by independent evidence, but it appears the most likely interpretation, given the geological and active-tectonic context and, what is known about eustatic sea-level fluctuations in the Mediterranean. Proving that the documented uplifts were abrupt (i.e., arguably coseismic), is equally difficult, but reasonably expected and rather probable. Five earthquakes in the last ca. 2000 yrs on the coastal fault zone responsible for the uplift, compare well with historical seismicity and the results of recent on-fault paleoseismological studies at the nearby Eliki fault zone. Exact amounts of coseismic uplift cannot be determined precisely, unless the rate of uniform ("regional") non-seismic uplift of Northern Peloponnesus at the specific part of the Corinth Rift is somehow constrained.

Using geomorphic and biological indicators of coastal uplift for the evaluation of paleoseismicity and Holocene uplift rate at the footwall of a normal fault (western Corinth Gulf, Greece)

N. Palyvos (1)(*), F. Lemeille (2), D. Sorel (3), D. Pantosti (1), K. Pavlopoulos (4)

(1) Istituto Nazionale di Geofisica e Vulcanologia, Rome, Italy,
(2) Institut de Radioprotection et de Surete Nucléaire, Paris, France,
(3) Université Paris-Sud, Orsay, France,
(4) Harokopio University, Athens, Greece
(*) now at (4)

Keywords: Holocene shorelines, Coastal fault zone, Coastal uplift, Paleoseismology, Shore platforms, Gulf of Corinth

Abstract

The westernmost part of the Gulf of Corinth (Greece) is an area of very fast extension (~15 mm/yr according to geodetic measurements) and active normal faulting, accompanied by intense coastal uplift and high seismicity. This study presents geomorphic and biological evidence of Holocene coastal uplift at the western extremity of the Gulf, where such evidence was previously unknown. Narrow shore platforms (benches) and rare notches occur mainly on Holocene littoral conglomerates of uplifting small fan deltas. They are perhaps the only primary paleoseismic evidence likely to provide information on earthquake recurrence at coastal faults in the specific part of the Rift system, whereas dated marine fauna can provide constraints on average Holocene coastal uplift rate.

The types of geomorphic and biological evidence identified are not ideal, and there are limitations and pitfalls involved in their evaluation. In a first approach, 5 uplifted paleoshorelines may be indentified, at 0.4-0.7, 1.0-1.3, 1.4-1.7, 2.0-2.3 and 2.8-3.4 m a.m.s.l. They probably formed after 1728 or 2250 Cal. B.P. (depending on the marine reservoir correction used in the calibration of measured radiocarbon ages). A most conservative estimate for the average coastal uplift rate during the Late Holocene is 1.6 or 1.9 mm/yr minimum (with different amounts of reservoir correction). Part of the obtained radiocarbon ages of *Lithophaga* sp. allows for much higher Holocene uplift rates, of the order of 3-4 mm/yr, which cannot be discarded given that similar figures exist in the bibliography on Holocene and Pleistocene uplift at neighbouring areas. They should best be cross-checked by further studies though.

That the identified paleoshoreline record corresponds to episodes of coastal uplift only, cannot be demonstrated beyond all doubt by independent evidence, but it appears the most likely interpretation, given the geological and active-tectonic context and, what is known about eustatic sea-level fluctuations in the Mediterranean. Proving that the documented uplifts were abrupt (i.e., arguably coseismic), is equally difficult, but reasonably expected and rather probable. Five earthquakes in the last ca. 2000 yrs on the coastal fault zone responsible for the uplift, compare well with historical seismicity and the results of recent on-fault paleoseismological studies at the nearby

Eliki fault zone. Exact amounts of coseismic uplift cannot be determined precisely, unless the rate of uniform ("regional") non-seismic uplift of Northern Peloponnesus at the specific part of the Corinth Rift is somehow constrained.

1. Introduction

An applied aspect of coastal geomorphology, concerns the contributions it can make to active tectonics and seismic hazard studies, be it e.g. quantification of long-term deformation rates (e.g. Burbank & Anderson, 1999), or, under favourable circumstances, the determination of past earthquakes that have not been instrumentally or historically recorded (paleoearthquakes, e.g. McCalpin, 1996). In some cases, geomorphological approaches may offer the only feasible, or the most cost-effective solutions for the extraction of quantitative information on Pleistocene-Holocene deformation and paleoseismicity.

Underwater coastal faults producing coastal uplift present such examples. The interaction between coastal geomorphic processes and an uplifting fault block, under favourable circumstances may lead to the formation and preservation of a readily identifiable geomorphic record of the uplift through time, consisting e.g. of uplifted paleoshorelines or marine terraces (e.g. Keller & Pinter, 1999). Dating of such uplifted marine features, provides estimates of the rate of coastal uplift, which can be used as input to mechanical models of fault dislocation for the estimation of the slip rate of the fault that causes the uplift (e.g. Armijo et al., 1996), slip rate being an important element for seismic hazard assessment. Furthermore, in tectonic coasts with Holocene uplifted features, the preservation of specific uplifted coastal landforms and associated bio-consructions can be shown to be the result of abrupt (coseismic) uplift caused by recent earthquakes (e.g. Laborel & Laborel-Deguen, 1994). In these cases, fossil shorelines correspond to invaluable records of earthquake reccurence at the fault responsible for the coastal uplift.

Studies on the above themes have been conducted worldwide, the more clear-cut and straight-forwardly informative cases being usually in areas of faster coastal uplift rates and larger earthquake magnitudes (i.e. larger coseismic vertical displacements of a given coast). Such areas are found at plate boundaries, like New Zealand or Chile (e.g. Lajoie, 1986), or Crete in the eastern Mediterranean, and are typically associated to very strong earthquakes ($M > 7$). Examples are also to be found though at smaller tectonic (seismogenic) structures, associated to smaller earthquake magnitudes, e.g. normal faults in intra-plate settings. Such case studies abound e.g. in the Mediterranean Sea (e.g. Pirazzoli, 2005).

This study concerns previously unknown remains of uplifted Holocene shorelines at the western part of the Corinth Rift in Greece (Figure 1), a major zone of seismic hazard in the Mediterranean. The shorelines are found in the area of fastest present-day extension, on the fast-uplifting footwall block of highly active coastal normal fault zones that are considered prone to rupture in the near future (Bernard et al., 2006). These uplifted shorelines are practically the only readily available primary field evidence that are likely to provide information on earthquake recurrence at the specific part of the Rift (primary, off-fault paleoseismological evidence in the classification of McCalpin, 1996). We will discuss uncertainties and possible pitfalls

involved in their paleoseismological interpretation, as well as the limitations in obtaining estimates of coastal uplift rate at the fault zone footwall, to provide a case study of problems that can be encountered in (or, may typify) the evaluation of similar, non-ideal evidence in similar active-tectonic settings.

2. Active tectonics context

The Corinth Rift ("CR" in the following) in central Greece (Figure 1) is the most rapidly extending area in Europe and the Mediterranean. Fast crustal extension reaches 14-16 mm/yr at the western part of the rift (e.g. Avallone et al., 2004) and is accompanied by highly active normal faulting on land and offshore. Associated seismicity is high, with abundant earthquakes (Ms 6-7) in the historical (Ambraseys & Jackson, 1997, Papadopoulos et al., 2000) and instrumental record (e.g. Tselentis & Makropoulos, 1986, Bernard et al., 2006).

The western termination of the WNW-ESE trending Corinth Rift, is defined by its intersection with the NE-SW Rion-Patras transfer system that is responsible for the formation of the Rion Straits (Doutsos et al., 1988, Doutsos & Poulimenos, 1992, Flotte et al., 2005) – Figure 1. The two fault systems (Corinth / Rion-Patras) are expressed by presently active coastal fault zones, namely, the Aigion-Neos-Erineos-Lambiri fault zone (ANELfz – Palyvos et al., 2005, "Kamares fault" in Bernard et al., 2006) and Rion-Patras fault zone (RPfz, e.g. Stamatopoulos et al., 2004, Flotte et al., 2005 – Figure 1). The Psathopyrgos fault zone (Pfz – e.g. Doutsos et al., 1988, Koukouvelas & Doutsos, 1997) is an E-W structure at the intersection of the Corinth / Rion-Patras systems.

All of the southern rift margin, i.e., the Northern Peloponnesus coast, is characterised by long-lasting uplift, as testified by uplifted Middle and Late Pleistocene marine terraces and marine deposits at both the eastern (e.g. Keraudren & Sorel, 1987, Armijo et al., 1996) and western part of the Corinth Gulf (e.g. De Martini et al., 2004, McNeil & Collier, 2004, Trikolas et al., 2004). Uplift is considered to be the combined result of fault footwall uplift (e.g. Armijo et al., 1996), including coseismic and associated interseismic movements, in combination with broader-scale ("regional") uniform uplift (e.g. Collier et al., 1992, Stewart & Vita-Finzi, 1996). Uniform uplift has been attributed e.g. to isostatic uplift above the low-angle subduction of the African plate under Peloponnesus (e.g. Collier et al., 1992, Leeder et al., 2003), or isostatic response to climatically-induced increase in rates of footwall erosion and hangingwall sedimentation (Westaway, 2002).

The North Peloponnesian uplift is a process active also during the Holocene. Geomorphological, biological, and sedimentological indicators of Holocene coastal uplift, although locally abundant, are in general rare and Holocene coastal uplift rates are generally not well constrained (Stiros, 1998). Previous works studying Holocene uplift are summarised in Figure 1 (coring/stratigraphic studies not included). At Platanos and Mavra Litharia (harbour of ancient Aigeira), Pirazzoli et al. (2004) have proposed the fastest Holocene uplift rates so far: 2.9-3.5 mm/yr at Aigeira, and possibly higher at Platanos, where the Holocene marine limit is at 11 m a.m.s.l. or higher. Platanos, is the the westernmost area where uplifted Holocene marine features were known until now.

The evidence of Holocene coastal uplift discussed herein are found along the NW part of the ANELfz (Lambiri f.z. –Lfz- see Pantosti & Palyvos, 2007a) and, to a lesser extent, the eastern part of the Psfz coastal fault escarpments (Figure 1 and Figure 2). This area, is characterised by the highest Late Pleistocene average uplift rates identified so far in the Rift (> 1.8 mm/yr), different estimates reaching up to 4 mm/yr or more (Stamatopoulos et al., 1994/2004)– see review in Palyvos et al. (2007a and in Pantosti & Palyvos (2007a).

3. Coastal geomorphological context and evidence of Holocene coastal uplift

The studied coast consists of a steep coastal escarpment comprised of uplifted Rift fill, namely Early-Middle Pleistocene alluvial fan conglomerates (e.g. Kontopoulos & Zelilidis, 1997) with marine deposits on its upper part (e.g. Doutsos & Poulimenos, 1992, Palyvos et al. 2007a) – Figure 2. Mesozoic bedrock consisting of thin-bedded limestones with some chert intercalations outcrops at the lower parts of the NW part of the escarpment. A steep escarpment has been recognised also underwater (Piper et al., 1990). Between locations 43 and 49, a fault-controlled limestone cliff more than 10 m high plunges into deep waters in front of it.

From location 43 to the SE, the base of the coastal escarpment is draped by coalesced small Holocene fan deltas, formed by small torrents. Those best expressed in the topography (with a fan-like shape) lie just to the east of Figure 2, near Lambiri village, which is built at the western edge of a much larger one associated to a major river (e.g. Piper et al., 1990). The ones within Figure 2 are less-well expressed due to the Lfz (or, a major, active strand of the Lfz) being just offshore, very near the coastline. The small catchment areas of the feeder torrents have not allowed for sedimentation rates fast enough to fill the accommodation space created by the Lfz (deep waters in front of the shoreline), inhibiting progradation and development of typical fan-like morphologies.

Holocene coastal uplift is indicated by emerged marine fauna and narrow (typically, 0.5-1.5 m wide) shore platforms (benches) and notches (e.g. Trenhaile, 1987, Pirazzoli, 1996). Such features have been widely employed in active tectonics studies in the Mediterranean, including those of the gulf of Corinth (e.g. Pirazzoli, 2005, Stiros & Pirazzoli, 1995). In most studies, the coastal bedrock is limestone, but notches and benches occur on other lithologies also, e.g. in conglomerates, at nearby Platanos (Stewart, 1996 – Figure 1).

The majority of geomorphic evidence of Holocene uplift is found on Holocene littoral conglomerates of varying coarsness. Depositional environments include paleobeaches, identifiable e.g. behind the small beach at Camping Tsolis (location 1 in Figure 2), where a conglomerate facies with characteristically flat and well sorted, cross-bedded pebbles is found -and a very well-preserved sea-urchin within it-, and in all probability, Holocene fan delta foreset slopes (Figure 3a). Given that progradation of deltas (worldwide) was generally possible only after the deceleration of Holocene SL rise, roughly since 8,000 – 6,000 years BP (e.g. Stanley & Warne, 1994), the above fan delta and associated beach conglomerates are expected to be younger than this age.

Some features occur also on outcrops of Mesozoic limestones and related underwater-deposited fault-slope scree (areas IV and V), which apart from angular

clasts derived directly from the bedrock, include also rounded gravel from the overlying Pleistocene conglomerates (Figure 3b-d). Man-made spoil from the construction of the Athens-Patras Railway line or national road is unfortunately ubiquitous, not permitting observations higher than 3-4 m a.m.s.l. in most cases.

4. Study methods

Benches and notches were surveyed with a tripod-mounted Zeiss Ni5 level and stadia. At locations where the use of tripod and stadia was not possible, elevation measurements were taken using a 1m builder's level and weight-suspended measuring tape, or, with Abney level and stadia. The horizontal distances in the profiles are in most cases only indicative. Locations of measurement sites were determined using handheld GPS (errors of +-5 to 7 m, depending on location).

Elevations were measured with reference to SL at the time of measurement (+-5-10 cm max error, larger in the case of the highest marine fauna and a sample dated in 2003 – see Table 2), and were adjusted to a common reference level based on tidal records from the Trizonia island tide gauge on the northern side of the gulf (indicated by "T" in Figure 1, data kindly provided by P. Bernard, IPGP), which is ca. 11 km away from the study area. Mean sea-level at Trizonia not being yet available, the reference level was the mean SL for the period 1995-2003 calculated by Milas (2003) based on records of a tide gauge at Galaxidi farther east in the Gulf, to which the measurements of the Trizonia tide gauge have been tied (P. Bernard, pers. comm.). The tidal range is small in the in the Gulf, about 15 cm on average (Poulos et al., 1996), although meteorological effects can cause significantly higher sea-level fluctuations (Milas, 2003). The tide is of the semi-diurnal type, with the amplitudes of the principal lunar component (M2) being 14.5 cm and of the principal solar component (S2) 9.5 cm at tide gauges at Galaksidi and Aeigira (Milas, 2003, based on tide-gauge data for the period 1995-2003). For comparison, spring tidal range was 47 cm at the Trizonia tide gauge in July 2005. No correction for atmospheric pressure changes and wind forcing is included in the measurements, which were taken preferentially during calm sea. At three locations, repeated measurements were taken during different campaigns and, after correction, the elevations above the reference level were found in very good agreement (within 5-10 cm).

Marine shells suitable for ^{14}C dating (AMS), were dated at the Poznan Radiocarbon Laboratory (Poland). Three of the dated samples were examined at light microscope and SEM prior to AMS dating, to exclude recrystalisation phenomena.

5. Survey results

Geomorphic evidence of paleoshorelines in different areas of the studied stretch of coast are summarised graphically in Figure 4 and described in the following. Features interpreted as true shore platforms (benches) are horizontal or sub-horizontal erosional surfaces either formed in homogeneous conglomerates and/or clearly discordant to bedding. Lack of structural control and hypsometric accordance with neighbouring benches were the criteria for the few notches identified as potential

SL indicators. Further discussion on the determination of past SL stand elevations from the notch and bench record will be given in the synthesis of survey results.

5.1. Area I

.

Narrow shore platforms (benches) and notches occur at 3 levels a.m.s.l. on littoral conglomerates in area I ("Camping Tsolis"). At location 1 (next to the staircase bringing to the cove and beach) the conglomerates are tilted away from the sea, indicating that Late Holocene tectonic or gravitational displacement has taken place. Profile 1 records a notch (2.8-3.0 m a.m.s.l. - Figure 5a) that is clearly discordant to the conglomerate bedding. The erosional surface the notch corresponds to, truncates both the cement and the cobbles of the conglomerate in a very smooth profile, indicating that abrasion was involved in its formation. A small bench with an inner edge at the base of the notch (dashed line in Figure 5a) can be followed a few meters to the southeast up to profile 3, where it is slightly higher (outer edge at 3.0 m). Profile 3 also records a well-defined notch, the base of which correlates hypsometrically to the intermediate bench at profile 1 and the upper bench at profiles 7/7b (Figure 5b). Profiles 7 and 7b record the step between two benches. Only the outer edge and part of the upper bench are preserved, at 1.7-1.8 m, whereas the inner edge of the lower one is at 1.0 m. The latter correlated to the lower bench at profile 1, which is higher than in profiles 7/7b, probably because it is capped by cemented beach material.

Profile 5 is from the NW side of the camping cove, where an apparently very well-defined bench and notch-like feature are preserved on a remnant of coarse conglomerate. The "notch" appears to correlate well with the bench level identified on the SE side of the cove. However, this morphology may be an artefact caused by deposition of younger beach material (now itself cemented) around an older conglomerate block, creating a "platform" that is not erosional but depositional.

A few m to the SE of location 5, always at the NW side of the camping cove, a strip of conglomerates is found in front of the shoreline (like a barrier island). Its landward limit is straight, suggesting that marine erosion was guided by a discontinuity along which recent cracking or, tectonic or gravitational displacements have taken place. This discontinuity is in front of the coast, thus it is not expected to have disturbed the continuity of the paleoshoreline remains along it. It projects however just behind the location of the backtilted conglomerates at profile 1.

5.2. Area II

Benches on Holocene conglomerates occur at 3 levels a.m.s.l. in area II. The 3 bench levels are best-defined and laterally extensive for several meters at the small stretch of coast corresponding to profiles 10-14 (Figure 5c). The inner edge elevations of the lower two benches are found at an average of 0.20 and 0.90 m a.m.s.l., respectively. During high waters, the lower bench is occupied even by small waves. Only the outer edge of the higher bench is preserved, at elevations of 1.90-2.0 m. At

the SE end of stretch 11-14, the stepped morphology of the coast becomes more complicated (profiles 10). At location 10 (SE end of stretch 11-14), a notch-like and small bench-like features that are not laterally extensive (1m or less) occur at different levels below the 2 m platform. They do not correlate with the very well defined bench levels immediately to their W. They are included with question-marks in Figure 4 as an example of features that we avoided interpreting as potential SL indicators. Similar, unpaired features occur at at profiles 15, 16 and 11.

At profile 9, a remnant of finer grained conglomerate records a well-defined sub-horizontal platform at ca. 0.7 – 0.8 m amsl. Profile 8 records a platform at ca 0.4 m, with a wide notch-like form in very coarse (cobble-grade) conglomerates. Farther west, well-defined benches exist at locations 17 to 19 at two levels (possibly, three). They are not included in the dataset, because of lack of tidal data during the period of measurement, due to malfunction of the Trizonia tide gauge data storage.

5.3. Area III

In area III, geomorphic evidence of up to 5 bench and notch levels can be found on Holocene conglomerates. Profile 41 (Figure 6a) depicts two very well-defined, sub-horizontal erosional benches in coarse conglomerate, with inner edge elevations at 0.5 and 1.5 m, whereas a third, higher bench (inner edge not visible) is found at 2.0 m. A notch is found at profile 39a at 0.65-0.75 m. Profile 39b records a bench at 1.35 m, a feature that is probably present -albeit not well expressed- also to the SE of 39b (area around profile 38). At profile 39c (behind profile 39a), the respective paleo-sealevel corresponds to a well-defined notch in coarse conglomerates (apex at 1.65-1.7m), which is discordant to bedding and quite deep (Figure 6b). The floor of this notch is only partly preserved.

Profiles 38-37 depict features observed along a few tens of metres of coast, immediately to the SE of location 39. Bench remains were observed at 1.0 m, and 1.55 m, whereas a wider bench with gently sloping morphology (not controlled by bedding), is found at elevations between 3.06 m (inner edge) and ca 2.91 m (outer edge). Three cauldron-shaped erosional features are carved into the bench, in cobble-grade conglomerates (clasts of 20x10-5 cm). They are circular in plan view, have vertical walls, diameter1.5 to 2 m, and depth of ca. 1m (CA in Figure 4 and Figure 6c). They are open at their seaward sides, and the lowest elevations of the openings are at a level of 1.83-1.90 m. The coincidence of the openings' lower elevations (Figure 6c) suggest relevance to a past SL stand. E.g. the cauldron bases may correspond to a former limit of permanent saturation (i.e. low tide level), above which the conglomerate cement was more weathered, allowing mechanical erosion to be more efficient and to form the cauldrons (see Trenhaile, 1987 for various physical and chemical processes that may be involved).

Location 35 is one of the cases where uplifted clinoforms (foresets) are best illustrated. Small erosional benches or steps on the emerged foreset slope are possible at different elevations (Figure 3a). The most convincing features were measured at three levels. At 1.45 m, a small bench remain (indicated with "C" in Figure 3a) truncates an isolated remnant of seaward-dipping conglomerates and a marine bioherm on them. On the SE side of the same conglomerate remnant, a lower bench is well-defined, albeit with irregular surface (elevation 0.6-0.7 m). At location 35a in the

same area, behind and just NW of 35, well-defined erosional levels exist at 1.0 and 0.6 m a.m.s.l. Possible higher features are discernible from the viewing angle in Figure 3a but, when looked at from various angles, they are rather inconclusive.

Location 32 records 3 bench levels (profiles 32b-d, Figure 6c) with inner edge elevations averaged at 0.6-0.7, 1.0 and 1.5 m. The 1 m bench corresponds to a possible true notch in very coarse conglomerates (profile 32a). A few meters to the east (profile 31), a lower bench at 0.5 m is well-defined, together with one at 1.9 m. Farther east, at profile 29 a small conglomerate block preserves bench remains at 0.5 and possibly also 0.7 m a.m.s.l. At Location 27 remains of a bioherm are found, truncated (?) by a possible erosional surface at ca. 3 m a.m.s.l. (buried by spoil).

5.4. Area IV

In area IV, coarse underwater-laid conglomerates consisting predominantly of angular cobbles (scree), drape Mesozoic limestone bedrock that outcrops most probably due to the existence of a fault exactly along the coastline (stretch 43-49 in Figure 2) - see Figure 3c/d. Marine erosion has produced a small cave along the bedrock / conglomerate contact at location 43 (Figure 7a). Here, the highest remains of emerged Holocene marine fauna *(Lithophaga* sp.*)* were found at an elevation of ca. 7.15 m, on a small outcrop of limestone bedrock some meters to the NW of the cave, amidst bushes and small trees (Figure 7b). The bedrock outcrop was rich in *Lithophaga* borings, a fact that may indicate vicinity to a paleoshoreline, but exposure was not adequately large to draw a safe conclusion. The steeply dipping conglomerates that constitute the roof of the cave are however truncated at a level around 7.2 m a.m.s.l., suggesting a SL stand at about this elevation. Higher fauna remains could not be found at location 43, because of colluvium and debris cover (the railway line is passing a few meters away from the outcrop and a retaining wall has been built a few meters higher the *Lithophaga* outcrop). Farther west, the terrain becomes too steep and we did not attempt to search (Figure 3d).

On conglomerate remains in front of the cave, a well-developed bio-herm is found up to 2.60m a.m.s.l., with thick *Spondylus* sp. shells and *Cladocora* sp. corals (Figure 7c), among the rich fauna it consists of. This bioherm is not a precise SL indicator and resembles very much the Holocene bioherms at Mavra Litharia (ancient Aigeira harbour – location in Figure 1) – see Pirazzoli et al., (2004) and Kershaw et al. (2005).

At location 43, a narrow bench is identifiable on the cemented conglomerates with an inner edge at 2.25 m a.m.s.l. whereas on the western side of the profile shown in Figure 7a, small benches occur at 1.35 and 0.6 m a.m.s.l. These benches are not included in the dataset because they were not paired with neighbouring features at the same location. The coastal cliff from location 43 to 49 remains unexplored at its steepest part. During a reconnaissance swim along it, we identified geomorphic evidence of a well defined paleoshoreline carved some meters above SL on a thick biogenic crust on scree and limestone (Figure 3d, not surveyed).

5.5. Area V

In area V, 5 bench levels are identified on littoral conglomerates, coarse to very coarse scree (boulders), and Mesozoic limestones. Profile 50 (Figure 8a) records

a well-defined notch at 1.5 m a.m.s.l. In front of the conglomerate remain with the notch, a strip (like a barrier island) of conglomerates is found in front of the shoreline, the landward limit of which is quite straight (strike N90^{o}E). As in location 5, marine erosion was guided here by a cracking or, a discontinuity that has hosted tectonic or gravitational displacements. However, also this discontinuity is in front of the coast, thus it is not expected to have caused lateral discontinuities in the bench record.

Profile 51b (Figure 8b) records a succession of 5 narrow sub-horizontal erosional benches in conglomerate that are not controlled by bedding. They occur at 0.3, 0.8, 1.3, 2.0 and 2.7 m. The inner edge of the highest bench is not preserved. At profile 51 (just west of 51b), the discordant relationship of the platform at 2 m with the seaward-dipping conglomerates is very clear.

Farther west, unambiguous evidence of erosional benches (without preserved inner edges) are found at location 52 and possibly 53. At 52, a platform remain, discordant on conglomerates, is found at ca. 1.55 m, whereas at 53, a coarse conglomerate promontory, a flat platform is found at ca. 1.1 m.

Location 54 is a small limestone promontory. Limestone is most exposed on the western side Figure 8c), whereas on the eastern side it is covered by a breccia composed of boulder-sized scree (Figure 3b), a material that has not permitted the formation of well-defined morphological features indicative of paleoshorelines. An open fissure corresponding to a structural discontinuity striking N80-105^{o}E and dipping to the N-NNE is also observable at the western side of the promontory (possibly, a neotectonic fault plane, but, not necessarily active in the Holocene). At the apex of the promontory (Figure 3b, Figure 8c), where limestone reaches higher elevations, no notches were observed. More or less pronounced steps do exist, at 1.69, 2.30 and 2.82 m, but they are not laterally extensive and do not pair with similar features nearby. A bench at about 1.64 m is possible though at the eastern side of the promontory.

At location 54, vermetid encrustations are abundant, but SL-critical species (e.g. *Dendropoma* sp.) were not identified, neither clear, laterally extensive horizontal zonations. Locally, upper limits of colonies of vermetids appear faintly possible at 1.67 m (eastern side of promontory) and at 2.27 m (western side, just outside Figure 8c), but specimens are rather sparse to draw safe conclusions. *Lithophaga* sp. borings are ubiquitous on the eastern side of the promontory, but on the western side, a band with upper limit at ca 1.3-1.5 m is possible (Figure 8c). No shells are preserved in the borings in this band. Inside the open fissure next to it, *Lithophaga* sp. shells are very well preserved, but it was unclear whether they belong to a colony with the same upper limit as the band outside the fissure.

At location 55 a remnant of a well-developed (flat) platform on limestone occurs at 1.95 m. At location 56 a thin remnant of beachrock is found at an elevation of ca 1.8 m, over a bench on bedrock. Below the beachrock, travertines are found around a fissure in the bedrock, but it is unclear whether the block with the beachrock may have been subjected to displacement (subsidence) in recent times. A small vermetid shell was found on the beach rock. This is the only case (apart from vermetids at location R in Figure 1) where we had an unambiguous relation between a vermetid (probably, *Vermetus* sp.) and a specific bench level.

Farther west, uplifted beach rocks (over Mesozoic limestone bedrock) are found at locations indicated by “BR” in Figure 2, at elevations generally below 2 metres (spoil masks the higher parts of the coast). From that area westwards, begins the stretch of coast in front of the Panagopoula landslide complex, where evidence of

uplift cannot be identified (due to lack of rocky coast, man-made modification and probably also because gravitational subsidence has interfered). From Panagopoula to Psathopyrgos, the only area where we found evidence of Holocene uplift was east of Rodini (R in Figure 1, see Pantosti & Palyvos, 2007b for detailed location & description).

6. Synthesis of survey results and identification of past sea-level stands

All recognised benches and notches are synthesised graphically in Figure 9. Excluding the few dubious features included with gray color in Figure 9, benches appear to be arranged in 5 levels above the reference level (labelled, A to E, reaching up to 3 m elevation). Good agreement between bench/notch levels in different locations is recognised. More so, considering that minor variations are reasonably expected, e.g. due to bench remains not having a perfectly horizontal inner edge, especially in the coarser (cobble-grade) coastal conglomerates, possible small differences in sea level between measurement sites and the Trizonia tide gauge due to atmospheric effects, small differences in the amount of recent coastal uplift at different sites, or local gravitational subsidence (of small magnitude).

The stretch of coast where all 5 bench and notch levels occur is labelled "A-A'" in Figure 2. In 4 of the bench levels, bench inner edge elevations coincide with the elevations of notch floors, and in one case (location 50, level C – Figure 8a), both features occur at the same profile. At location 51 (Figure 8b) all 5 bench levels (A to E) are found at a single profile and at location 35 the lower 4 ones very close to each other. These locations exclude the possibility that the 5 bench levels may be an artefact caused by vertical dislocations (gravitational, or by secondary strands of the Lfz) of a smaller number of bench levels.

Using the bench and notch record for the inference of past SL stands, requires the identification of their relationship to mean SL (MSL) at the time of their formation. This necessitates identification of the processes that are responsible for their formation, or comparison with presently active, similar geomorphic features at the same location, which ideally should be the reference with respect to which the elevations of uplifted benches and notches are measured (Pirazzoli, 1996). In our case, present-day benches and notches in stretches of shoreline not concealed by beach gravel were either absent or, ill-defined and not identifiable beyond doubt as non-structurally controlled erosional features. This is so, accepting that the MSL identified by Milas (2003) at Galaxidi (the datum the measurements ultimately refer to) is the MSL also at our coast. Most of the lower benches we identified are substantially higher than this MSL. Thus, in order to identify the most likely relationship between bench and notch elevations with the elevations of past SL stands, it is necessary to resort to comparisons with well-documented analogs (contemporary or fossil), in neighbouring, similar coastal environments, where formation processes may be expected to be similar.

Among the various genetic types of notches (structural, abrasion, surf, tidal notches), tidal notches, whose formation is attributed mainly to bio-erosion processes in limestone (carbonate) coasts, are the most precise geomorphic SLI (e.g. Pirazzoli,

1996, Kelletat, 2005b) in microtidal areas such as the Mediterranean (tidal range typically <0.5 m). The apices (or retreat points) of tidal notches correspond to MSL, where erosion rate is highest, whereas their height closely approximates the tidal range (e.g. Pirazzoli, 1996/2005). The few notches discussed herein occur on conglomerates rich in carbonatic cement and limestone clasts, whereas their heights compare well with the tidal range. That these conglomerates are subject to bioerosion is also directly verified, by the abundance of *Lithophaga* sp. perforations on both their matrix and clasts. Notch-forming processes other than bioerosion are expected to be involved however, at least in the case of the 3 m notch at profile 1. Here, abrasion should be evoked to explain the perfecty smooth, polished form of the interior of the notch.

In the microtidal coastal environments of the eastern Mediterranean, as Pirazzoli (2005) discusses, good geomorphic SLI are the almost horizontal benches (i.e. narrow horizontal shore platforms) formed in the inter-tidal zone, often ending landwards being the floor of a tidal or an abrasion notch. Always according to Pirazzoli (2005), such benches usually tend to to be lowered to the low tide level, and often develop in gently-sloping limestone coasts or, in softer rocks where a notch profile may not be preservable. Contemporary examples of such narrow, sub-horizontal benches in the lower intertidal zone, in combination with notches or not, are known e.g. from Kefallinia Island (limestone coast, to the NW of and not far from our study area – Pirazzoli, 2005), Calabria (on sandstone - Pirazzoli et al., 1997), or western Peloponnesus (on calcareous sandstones – Maroukian et al., 2000 and unpubl. data). At location "R" in Figure 1, the only place where we identified a well-developed contemporary platform in the broader study area, it was also located below MSL (formed on thin-bedded limestones).

The elevation and gradient of shore platforms with respect to MSL is controlled by tidal range, wave climate, weathering environment and coastal lithology (e.g. Trenhaile, 1987/2002). Pirazzoli et al. (1997), referring to narrow benches at the lower intertidal zone in Calabria, mention that they usually result from the removal by waves of already weathered parts of coastal rocks, the lowest level of possible weathering corresponding to that of constant soakage by sea water, probably in the intertidal zone. This explanation complies with the literature on Australasian platforms, where weathering is considered the dominant process (e.g. Trenhaile, 1987/2002). Trenhaile (2002) doubts the presence of an abrupt change in water content above a well-defined level within the intertidal zone, identifying a gradual transition in the degree of weathering within the intertidal zone. He also summarises works demonstrating that waves can cut quasi-horizontal platforms in low tidal range environments, acknowledging though the contribution of weathering above the low tidal level (below which the rock is permanently saturated) in the formation of platforms at the low tidal level. Furthermore, he identifies that weathering may be a dominant influence on the development of narrow shore platforms in resistant rocks in sheltered environments.

In microtidal coasts exposed to strong waves, sub-horizontal platforms higher than MSL or even the high tide level may form (e.g. Kennedy & Dickson, 2006). Platform elevation may vary significantly within short distances in the same coast, particular being the influence of the vulnerability of coastal rock as determined by joints, faults and bedding planes, its compressive strength, and shoreline water depth (e.g. Thornton & Stephenson, 2006, Kennedy & Dickson, 2006). Increasing strength and water depth is associated to higher platform elevations, increasing rock vulnerability

to lower elevations. However, in the eastern Mediterranean, where surf action is moderate, Pirazzoli (1996) reports that "surf benches" (or "trottoirs") in limestone coasts are usually found no more than 0.2 to 0.4 m a.m.s.l. (see also Trenhaile, 1987 for examples). In the western Mediterranean (Mallorca), platforms much wider than the benches herein, in coasts exposed to stronger waves, lie close to mean SL and more specifically, within the intertidal zone (+-20 cm around MSL - Gómez-Pujol et al., 2006 and pers. comm.).

Considering that: a) our coast is in an enclosed gulf, where wave intesity is expected to be smaller compared to the average eastern or western Mediterranean coast**,** b) the lack of substantial variation in the elevations of benches and correlative notches along stretch A-A' but also to its east and**,** c) bench examples in the vicinity of the study area, it appears most likely that the narrow benches herein were formed very close to MSL and in the lower part of the intertidal zone. In Figure 4 and Table 1 include paleo-SL elevation estimates that are derived if benches are assigned to the lower part of the intertidal zone and notch apices to MSL. These values are indicative; true values may be somewhat lower (but, expectedly in a systematic way), for the reasons discussed previously. Colored bands in Figure 4 and Figure 9 approximate paleo-intertidal zones, their thickness complying to a spring tidal range of ca. 47 cm at the Trizonia Tidal gauge in July 2005.

We do not consider the possibility of multiple benches forming with respect to a given SL stand, since platforms formed by storm wave erosion or salt-weathering above those closely related to the mid-littoral zone (e.g. Trenhaile, 1987, Bryant & Stephens, 1993) are expected to show variance in their elevations from location to location, something that lacks our dataset in stretch A-A'. A further, strong argument comes from location "R" in Figure 1 (see Pantosti & Palyvos, 2007b), where a contemporary platform on limestone is well developed below MSL, and a second one, partly covered by beachrock lies at 0.4-0.5 m a.m.s.l. On the 0.4-0.5 m bench, dead vermetids were found. These organisms live just below MSL (e.g. Stiros et al., 2000) and thus indicate that the 0.4-0.5 m platform cannot have the same age as the contemporary one.

7. Radiocarbon dating

Whereas uplifted marine fauna is at several locations abundant, it proved very difficult to correlate marine fauna remains with specific paleoshorelines, with very few exceptions. This is due to absence of littoral bio-constructions or fauna assemblages indicative of a paleo-mid-littoral zone in unambiguous association to the surveyed notches and platforms (e.g. Laborel & Laborel-Deguen, 1994, Stiros et al., 2000). Rare exceptions of fauna with a clear relationship to specific paleoshorelines, were gastropods in cemented material (beachrock) that we could discern to be different that the conglomerate "bedrock" on bench D at location 10 (possibly also 51), and a small vermetid tube on the beachrock at location 56.

Potential pitfalls that had to be avoided, relate to the fact that the dominant bedrock, i.e. the Holocene conglomerates, which were deposited underwater, contains Holocene fauna itself. E.g. in favourable exposures pebbles and cobbles that were perforated by *Lithophaga* before the conglomerate cementation were observed (the cement was covering the borings and the shells inside them). Such *Lithophaga* pre-

date the erosion that produced the surveyed geomorphic features. In other cases, vermetids (not SL-critical species) that lived in open spaces of cobble-grade open-work conglomerates soon after their deposition, may be well-preserved, and "fresh-looking" when exposed by erosion, and mis-interpreted as fauna that post-dates the formation of geomorphic features that are instead younger. In addition, in paleo-littoral zones where narrow cobble or pebble beaches were present (equivalent to those observed today), cobbles with SL-critical fauna attached to them may have ended up at larger depths by rolling down the steep submarine slope, which typically begins only a few meters from the shoreline. This is a characteristic configuration in the present-day small beaches. Such out-of place cobbles may be encountered after uplift in the emerged conglomerate bedrock, a possibility that increases the importance of finding several SL-critical organisms in a well-defined bio-zonation level.

In addition to the above, in the Corinth gulf, a major problem in dating accurately Middle-Late Holocene marine organisms is the lack of a well-constrained local correction factor (ΔR) for the reservoir correction (e.g. Pirazzoli et al., 2004). Pirazzoli et al. (2004) apply both of the two extreme ΔR estimates of +380 (used by Soter, 1998) and -80 yrs (following Stiros et al., 1992). The range between these values includes ΔRs determined by Reimer & McCormac (2002) for nearby Hellenic seas. This results in broad calibrated age ranges. Furthermore, the youngest of the features that we would like to date, are expected to be a few centuries old, where calibration of conventional radiocarbon ages in any case yields very wide calendar age ranges, due to "plateaus" in the calibration curve (Hughen et al., 2004, and older curves).

All the above, suggest that dating specific shorelines with enough precision is very difficult and in any case, obtaining trustworthy results would require a (large) number of datings not possible in this study. In order to provide at least a crude chronological framework for the shorelines, but also to obtain constraints on the Holocene coastal uplift rate (a minimum estimate), 6 *Lithophaga* sp. shells from different elevations at the same location (location 43) were dated. Location 43 is unique in that uplifted Holocene marine fauna is not buried by spoil up to an elevation of ca. 7 m, and in addition, here sample fauna that was for sure in situ could be sampled on limestone bedrock. This way, possible pitfalls discussed earlier, which could lead to minimum uplift rate estimates much smaller than true values, are avoided. The dating results are summarised in Table 2 and plotted against elevation in Figure 10a

Of the samples dated, samples 43/3A, 3C and 43/2003 were examined at a SEM for recrystalisation or indications of alteration at IRSN and BRGM (respectively), before being sent for dating. The rest of the samples were examined only macroscopically. In the following, we discuss the constraints that the dating results provide for the ages of the identified paleoshorelines and the coastal uplift rate, together with the interpretive problems involved.

7.1. Constraints on the age of the paleo-shorelines

The surveyed benches and notches should be younger than ca. 6-8 ka, considering that they have formed on paleobeach or foreset conglomerates of Holocene fan-deltas that were expectedly able to prograde only since that time (Stanley & Warne, 1994). This way, the possibility that some of the paleoshorelines may correspond to Holocene SL stillstands pre-dating the deceleration of SL rise can be excluded. Such shorelines (submerged notches) have been described e.g. by Collina-Girard (1999) in stable coasts of the western Mediterranean. The shallower of these features, at -11 and -17m below m.s.l., would be emerged today considering the minimum uplift rate that will be estimated later on for our coast, but their remains would be expected only on exposures of bedrock limestones (perhaps also in scree).

Tighter constraints on the recency of paleoshorelines E to A can be provided if the maximum age of the *Lithophaga at +3m* (sample 43/2003) is considered a maximum-limiting age for the ca +3m (E) and lower paleoshorelines. This can be so, because the 3m *Lithophaga* lived at a time when relative SL (RSL) was 3m or higher above present MSL. The maximum ages of sample 43/2003, for ΔR = -80 and 380, would place the formation of the paleoshorelines after 2298 or 1728 Cal. BP, respectively. However, since the *Lithophaga* was not part of a fossil assemblage that could be firmly associated to the +3 m paleoshoreline, such a conclusion depends on the assumption that eustatic SL rise (or subsidence of the coast) did not cause a relative SL rise of enough magnitude to exceed the ca. 3m paleoshoreline after its formation and abandonment. In such a case, the latter could be older than the dated *Lithophaga*. In section 7, there is further discussion on this likelihood.

7.2. Constraints on the average coastal uplift rate during the Late Holocene

Because *Lithophaga* can live in depths down to 20-30 m, they are generally not accurate SL indicators, except when their distribution in an appropriately large rock exposure shows a well-defined upper limit, and particularly if this upper limit corresponds to the apex of a littoral notch or to the outer flat of an intertidal platform (e.g. Pirazzoli et al., 1994, Laborel & Laborel-Deguen, 1994). The samples between 3 and 4.8 m do not obey these conditions, whereas we didn't have an appropriately large exposure to confidently ascertain whether this might be the case with the 7.15 m samples. Thus, the average uplift rate (AUR) estimates that will be obtained should be considered minimum values.

The present elevation of the dated *Lithophaga* is the resultant of eustatic SL change due to ice melting, regional glacio-hydro-isostatic movements of the crust, and tectonic or gravitational movements of the specific coast (e.g. Lambeck & Purcell, 2005). Minor(?) contributions due to oceanographic and climatic forcing of the ocean surface (e.g. Mörner, 2005) can be a further component. Thus, in order to obtain an estimate of the AUR, i.e. the tectonic contribution to relative SL (RSL) change at the specific coast, the eustatic and glacio-hydro-isostatic contributions to SL change need to be constrained. At present, the best way to do this would be to use a SL curve from a tectonically stable area in the same broader region, i.e. an area where the glacio-hydrostatic contribution would be the same. Unfortunately, very few areas in Greece

may be considered tectonically stable (if any), and there is no "stable coast" where more than a few accurate markers of former SL stands have been accurately dated. A high-resolution SL curve for Greece –with 0.25 m accuracy or higher- practically does not exist, especially for periods older than 6000 yrs BP. For example, Pirazzoli et al. (2004) use the curve of Bard et al. (1994) from Tahiti, to estimate the AUR at Mavra Litharia. Furthermore, the peninsular shape of mainland Greece, is expected to result to important differences in hydro-isostatic contributions to SL change along its coasts (see e.g. model of Lambeck & Purcell, 2005), complicating correlations between different datasets.

In the following, a minimum value for the AUR will be obtained by comparing our dataset with SL datasets based on field data and, with the model of Lambeck & Purcell (2005). We will use the curves of Laborel et al. (1994), included with additional datapoints in Morhange (2005) (from dated littoral bio-constructions / archaeological data – Cote d' Azur, NW Mediterranean) and, for periods older than 6000 BP, the curves of Bard et al. (1996) (corals at Tahiti and Guinea). The curves of Bard et al. are employed following Pirazzoli et al. (2004), to facilitate comparison with their results at Platanos and Mavra Litharia.

We note that, according to the model of Lambeck & Purcell (2005), in the area of the Laborel et al. / Morhange curve, the glacio-hydroisostatic contribution to SL change would be very close to the one in our study area (they fall on the same contours in the SL maps of Lambeck & Purcell). Given that the coast where the Laborel et al. curve comes from has been subjected to negligible tectonic movements in the period of interest (Lambeck & Purcell, 2005), it would be a curve well-suited to derive the tectonic component of SL change at our coast. This conclusion is perhaps too good to be true, since it considers that the model of Lambeck & Purcell is absolutely correct in the area of Greece (see e.g. Pirazzoli 2005b for objections).

Minimum AUR estimates from the lower *Lithophaga* samples. Table 3, includes minimum AUR estimates based on each of the 4 lower *Lithophaga* samples separately, applying corrections for paleo-SL based on the SL dataset of Laborel et al. / Morhange and the model of Lambeck & Purcell (2005). The AUR estimates range between 1.5 and 2.4 mm/yr (including both extreme ΔR values used in the radiocarbon age calibrations). The estimates based on the 3 m *Lithophaga* appear as possible "outliers" in the dataset, which is though rather too small to be sufficient to cast doubt on the specific age. It can be that the 3 m *Lithophaga* was living closer to SL than the other samples.

The minimumAUR estimates would be slightly lower, if other SL curves are used, e.g. the curve of Flemming & Webb (1986). Conversely, SL curves that in the period of interest are substantially steeper than those used herein, have been proposed based on field data in various areas of Greece (e.g. Fouache et al., 2005, or Kelletat, 2005). Such curves would yield substantially higher AUR estimates than those in Table 3.

Figure 10b depicts a best-fit, extremely conservative estimate of minimum AUR, using the SL dataset of Laborel et al. / Morhange for paleo-SL correction. Each of the 4 lower *Lithophaga* is represented by two points, corresponding to maximum and minimum age, connected by lines. Triangles and squares distinguish data points based on age calibrations with ΔR of -80 and 380, respectively. The data points have been « pulled down » at the slowest possible rates that allow them to graphically coincide with the SL dataset of Laborel et al. / Morhange. Points lying below the SL dataset are allowed, because the *Lithophaga* were living at an unspecified depth below

sea level. Points above the SL dataset are not. However, we chose to allow the 3 m *Lithophaga* to be -only slightly- an outlier, lying just above the SL dataset, so that the obtained min. AUR estimate relies on more than just one dating. The minimum AUR thus derived, is of the order of 1.6 or 1.9 mm/yr (for ΔR -80 and 380, respectively), a figure that compares well with minimum Pleistocene AUR estimates of 1.8 mm/yr for the broader area (Palyvos et al., 2007a). Much smaller estimates (0.7-0.8 mm/yr - Houghton et al., 2003) do not contradict the results herein, because they refer to a block at the intersection of the Rion-Patras and Psathopyrgos fault zones and do not have a regional significance (Palyvos et al., 2007a/b).

Minimum AUR estimates using the higher *Lithophaga* samples. Figure 10c includes the SL datasets of Bard et al. (1996) for Tahiti and Guinea. The Tahiti dataset practically coincides with the eustatic SL curve predicted by the model of Lambeck & Purcell (2005) at our study area (Figure 10c). The youngest *Lithophaga* sample yields AURS of 3.0-3.7 mm/yr and 3.8-4.4 mm/yr, using the Guinea and Tahiti dataset, respectively (Table 3). Figure 10c depicts the scenario based on the Guinea dataset. The AUR estimates become 3.7-4.2 mm/yr and 4.5 – 4.9 mm/yr for Guinea and Tahiti (resp.), if the age of the oldest *Lithophaga* is used (Table 3).

Pleistocene AUR estimates of the order of 4 mm/yr or more do exist in the bibliography for the coast 10-15 km to the west of the study area (Stamatopoulos et al., 1994/2004), but, perhaps should better be verified by more data (see Palyvos et al., 2007a/b). Very high Holocene uplift rates (>2.1, or 2.9-3.5 mm/yr) are reported also farther E, at the uplifted harbour of ancient Aigira (Stiros, 1998, Pirazzoli et al., 2004). Thus, the AURs derived from the two 7.1 m Lithophaga cannot be discarded, but certainly need cross-checking.

8. Interpretation of the paleo-shoreline record

Following examples in e.g. Pirazzoli et al. (1999), the paleoshoreline data will be discussed in the context of changes of relative sea-level (RSL). As the studied coast is uplifting, it is characterised by a general trend of RSL fall (Figure 10a). Coastal uplift is the product of coseismic fault footwall uplift, superimposed or not on an unknown amount of uniform ("regional") non seismic uplift. Coseismic uplift episodes would correspond to episodes of abrupt RSL fall.

The presence of sub-horizontal benches (and few well-defined notches), suggest that the RSL history of the coast involves RSL still-stands, separated by changes in RSL that have been fast enough to allow the preservation of the above geomorphic features. In the term "RSL still-stand" we include for the sake of simplicity periods of very slow RSL change (that would permit the formation of sub-horizontal benches). RSL stability or very slow change may be due to SL stability, or due to the rate of SL rise equaling the rate of non seismic coastal uplift. The RSL still-stands are drawn as horizontal bars in Figure 11a-b, in different scenarios of timing, constrained only by the maximum possible ages of the dated *Lithophaga* at 3m (two calibrations, solid and dashed vertical lines). The length of the bars, i.e. the duration of the still-stands, is only schematic (arbitrary).

Given the general trend of RSL fall (coastal uplift), the resultant of RSL changes between RSL still-stands should be RSL fall. Yet, it cannot be assumed that all RSL changes correspond to RSL falls (Figure 11a), unless all of the shorelines are

dated and demonstrated to be successively older with increasing elevation**.** Thus, the possibility of younger shorelines occuring higher than older ones (Figure 11b), due to episodes of RSL rise superimposed on the general trend of RSL fall (e.g. Pirazzoli et al., 1999, 2004), needs to be considered. RSL rise could be caused by either subsidence of the coast or, eustatic SL oscillations, the likelihood of each we discuss in the following. .

Coastal Subsidence. Possible RSL rises due to coastal subsidence, may correspond to episodes of tectonic (coseismic or non-seismic) or gravitational (landslides) subsidence. Large-scale gravitational phenomena are known along the Psfz coastal escarpment (e.g. Koukouvelas & Doutsos, 1997). On the stretch of coast of interest herein, i.e. stretch A-A' in Figure 2, recent landslides are much smaller though (e.g. Rozos, 1991), and apparently limited to the Pleistocene alluvial fan gravel and marine deposits at the upper part of the coastal escarpment, (e.g. area indicated by "L" and question mark in Figure 2). At any rate, the good correlation of benches along stretch A-A' (Figure 9) indicates that after the formation of the benches, landsliding has not taken place at the measurement sites.

Coastal subsidence episodes of tectonic nature may be either co-seismic, or non-seismic. In the former case, the cause would be displacement along a strand of the Lfz on the landward side of the coastline. Such faults are expected along the base of the escarpment behind the fan-deltas. Two fault outcrops exist at location A in Figure 2, and a man-made cut inside the village of Lambiri, SE of Figure 2 (Pantosti & Palyvos, 2007a/b). However, the most active strand of the Lfz is expected to be the one right in front of the coast (offshore), otherwise Holocene shorelines would submerge, rather than uplift at a fast rate. Even if it is assumed that coseismic displacement on an onshore (secondary) fault strand may have caused a decrease of the net RSL fall caused by the active fault zone on the seaward side of the shoreline, or even net RSL rise (i.e. coastal subsidence), it appears rather unlikely that it may have done so in a homogeneous way, all along stretch A-A', without disturbing the regularity in the elevation distribution of bench remains (Figure 9). Thus, we do not favour a scenario including coseismic RSL falls, which, in any case would indicate activation of the Lfz, changing nothing regarding the potential paleoseismological significance of the paleoshoreline record (see later discussion).

Non-seismic (gradual) tectonic displacements of shorelines, often in opposition to the coseismic ones, may occur during the few years or decades preceding or following a seismic event (e.g. Pirazzoli et al., 1999). The nearest documented example, is gradual pre-seismic subsidence associated to the Kefallinia earthquake of 1953 (Laborel & Laborel-Deguen, 1994), and was identified on the basis of vermetid encrusters. I.e., the pre-seismic subsidence left no geomorphic imprint whatsoever. This suggests that such short-lived, transient phenomena are rather unlikely to have had an impact on our geomorphic record of paleoshorelines, because formation of metre-wide benches would necessitate RSL stability for more time than just a few decades.

Eustatic sea-level oscillations. Eustatic oscillations of the Late Holocene SL above present MSL (apart from a Middle Holocene highstand that is generally accepted for the southern hemisphere) have been proposed based on field data e.g. in Sweden and Maldives (Mörner, 2005 - Figure 12a), Australia (Baker & Haworth, 2000), and the Black Sea (Chepalyga, 1984, in Kelletat, 2005). Mörner (2005, and previous works) summarises possible mechanisms that can cause high-frequency,

metre-scale SL oscillations, e.g. redistribution of ocean waters after ice melting finished, or climatic changes causing changes in evaporation and precipitation.

Regarding the Mediterranean, to our knowledge the highest-resolution Late Holocene SL curve is that of Laborel et al. (1994) / Morhange (2005) for the the Côte d' Azur (France), a coast that is considered tectonically stable - Figure 12b. This SL dataset indicates a gentle SL rise in the last 3,000 ka, with SL oscillations (i.e. peaks in the curve) smaller than 0.35 m in amplitude. That is, SL oscillations in the western Mediterranean in the Late Holocene appear to have been much smaller than elsewhere (curve in Figure 12a is also plotted in Figure 12b for comparison). This suggests that they are unlikely to be relevant to our shoreline record, where we have shorelines spaced every 0.5 m or more from each other (based on profile 51b, where all shorelines –A to E- are present).

Putting SL oscillations aside, RSL changes in our coast may include RSL rises that correspond to periods of accelerated SL rise (i.e. steeper segments in a gently rising SL curve). In the period of interest, in the Morhange (2005) dataset there is actually possibility for such a fast SL rise of the order of 0.5 m, at around 1750 BP (cyan dashed line inside green rectangle in Figure 12b). On the other hand, this step is not evidenced in the Laborel et al. (1994) dataset. The Laborel et al. dataset also does not exhibit the 1.10m of SL rise between the 12th and 14th centuries AD reported by Ge et al. (2005) at the French Atlantic coast (Bordeaux), which thus may not apply to the Mediterranean.

The above is what we can say based on the available data, noting though the uncertainties introduced by using a SL dataset from a different area in the Mediterranean, where the history of Late Holocene SL change may be somewhat different. More specifically, Mörner (2005) predicts that the Aegean Sea could have an increased sensitivity to climatically induced SL fluctuations.

Preferred Interpretation. Keeping all the above considerations in mind, until higher-resolution ESL data become available for Greece and a more constrained chronology of the paleoshorelines under discussion is somehow established, based on the characteristics of the Laborel et al. / Morhange dataset, it appears more likely that the RSL changes between the RSL still-stands in our paleoshoreline record do not include RSL falls. I.e. our preferred interpretation is that all RSL changes are falls, reflecting episodes of coastal uplift (Figure 11c/d). This would place 5 episodes of coastal uplift in the last 2300 or 1750 yrs.

Paleoseismological significance. If uplift episodes can be demonstrated to be episodic, i.e. coseismic, the paleoshoreline record attains paleoseismological value. Several of the studies in the Corinth Gulf (listed in Figure 1) include or are devoted to this theme. Abrupt, arguably coseismic uplift of a paleo-shoreline is best established by convergence of different indications: biological, geomorphological, stratigraphic, historical and archaeological – Pirazzoli (1996, 2005). Perhaps the most convincing stand-alone evidence is the presence of well-preserved uplifted frail skeletal remains of marine organisms that have escaped mid-littoral erosion (e.g. Laborel & Laborel-Deguen, 1994, Stiros et al., 2000), including well-preserved *Lithophaga* sp. shells inside their burrows (e.g. Stiros et al. 1992). Testimony of abrupt uplift can also be the good preservation of morphological SL indicators, i.e. well-defined notches, with preserved floors and associated platforms, although, geomorphic evidence alone may be ambiguous (e.g. Pirazzoli, 1996, 2005).

Coseismic uplift of the paleoshorelines herein can be proposed, but not irrevocably proved, based on the preservation of well-defined benches and –fewer- notches, considering that the lithology where these features are found in our coast (conglomerates) is more easily erodible than limestones (where typically such features occur - e.g. Pirazzoli 1996, 2005, Kershaw & Guo, 2001). An additional, indirect argument is the geodynamic context, with the paleoshorelines lying at the footwall of active normal fault zones, in the area of fastest present-day extension in the Corinth Rift, within which coseismic shoreline uplift by coastal normal faulting has been identified in several locations (all areas of previous works, in Figure 1). Five strong earthquakes in the last ca. 2000 yrs, is not an exaggerated figure, considering the results of on-fault paleoseismological studies at the neighbouring Eliki fault zone (Pavlides et al, 2004, McNeill et al., 2005). The latest results (Koukouvelas et al., 2005) indicate 4 earthquakes since ca. 1600 BP. Also the historical record of strong earthquakes (Ambraseys & Jackson, 1997, Papadopoulos, 2000) contains abundant events in the last 2000 yrs with epicentral areas allowing correlation with the fault zone along the studied coast.

If the hypothesis of coseismic uplift episodes is accepted, the amount of coseismic uplifts would be important to determine, since it can be used as a parameter in dislocation modelling (e.g. Armijo et al., 1996) to determine the magnitude of the causative earthquakes. One factor that can introduce uncertainty in this case is that the paleoshoreline record need not necessarily record all uplift episodes, e.g. because small uplifts may have not uplifted erosional features above the inter-tidal zone (thus, not allowing their preservation), or uplifts spaced close in time may have not allowed for the formation of distinct erosional features. E.g. the 1m elevation difference between shorelines D and E may not by default correspond to one episode of uplift. Furthermore, coseismic uplift is superimposed on an unknown amount of non-seismic, uniform uplift of the Northern Peloponnesus (e.g. Stewart & Vita Finzi, 1996), the true rate of which remains to be somehow constrained. In different combinations of non-seismic uplift rate (including no non-seismic uplift) and rate of SL rise, the amount of coseismic uplifts can be smaller, equal to, or larger than the elevation difference between the successive paleoshorelines (Figure 11c and d). A comment that can be made, is that, in order to explain the presence of RSL still-stands that are necessary for the formation of benches, non-seismic "regional" uplift rate should perhaps be close to the rate of Late Holocene SL rise. The latter though, is also not well-constrained in the specific area, at the moment.

9. Conclusions

Geomorphic and biological evidence of Holocene coastal uplift at the footwall area of an active coastal fault zone, are identified at the rapidly extending western extremity of the Corinth Gulf Rift, where they were previously unknown. This evidence comprises narrow, horizontal shore platforms (benches) and notches, mainly on Holocene littoral conglomerates of uplifting small fan deltas. The interpretation of this evidence in terms of exact past relative sea-level stand positions and the nature of the intervening relative sea-level changes (uplift/subsidence, abrupt/gradual), involves uncertainties stemming from lack of precise knowledge of the exact processes

involved in bench formation, the lack of associated precise biological indicators of sea-level and, of detailed chronology of the uplifted benches and notches.

In a first approach, the more likely interpretation of the non-ideal record of uplift at hand indicates 5 paleo-shorelines, at 0.4-0.7, 1.0-1.3, 1.4-1.7, 2.0-2.3 and 2.8-3.4 m a.m.s.l. at the area where the Lambiri f.z. intersects with the Psathopyrgos f.z. Based on the interpretation of obtained radiocarbon ages, these paleoshorelines probably formed after 1778 or 2250 Cal. B.P., depending on the marine reservoir correction used in the calibration of the measured radiocarbon age (the local correction factor ΔR is poorly constrained in the Corinth Gulf).

A most conservative estimate for the average coastal uplift rate during the Late Holocene is that it has been higher than 1.6 or 1.9 mm/yr, depending on the amount of reservoir correction applied to radiocarbon ages. Just how much higher the true value may be, cannot be resolved with the ambiguities in the available data (lack of exact sea-level indicators, uncertainties in the reservoir correction that needs to be applied in radiocarbon ages, lack of a high-resolution eustatic sea-level curve for the area). Two of the obtained radiocarbon datings, coming from the highest *Lithophaga* retrieved, allow for much higher uplift rate estimates, of the order of 3-4 mm/yr, which we hesitate endorsing though, until more data provide cross-checking.

That the paleoshoreline record corresponds to episodes of uplift (relative sea level fall) only, has not been demonstrated by independent evidence, but it appears the most likely interpretation, given the geological and active-tectonic context, and what is known about eustatic sea-level fluctuations in the Mediterranean. Proving that the documented uplifts were abrupt (i.e., arguably coseismic), is equally difficult. However, given that the paleoshorelines are at the footwall of an active normal fault zone that passes right in front of the coast, in the area of fastest present-day extension in the Corinth Rift, the above hypothesis appears the most likely one, indicating 5 probable earthquakes in the last ca. 2000 yrs. The exact amount of coseismic uplifts cannot be determined precisely, unless the rate of "regional" non-seismic uplift of Northern Peloponnesus at the specific part of the Corinth Rift is somehow constrained. The identification of relative sea-level still-stands (or, periods of very slow relative sea-level change) in the coastal uplift history, which are necessary for the formation of sub-horizontal benches, indicates that the rate of non-seismic ("regional") uplift should perhaps be close to the rate of eustatic sea-level rise.

10. Acknowledgements

This study was carried out in the frame of the 3HAZ Corinth E.U. research project. We are grateful to Pascal Bernard (IPG Paris) for providing us with tidal data from the Trizonia tide gauge, Jacques Philippon (DRAC, Lille) for SEM analyses and Thomas Goslar (Poznan Radiocarbon Laboratory) for always being available to answer our questions about the interpretation of dating results. We also thank Kostas Tsolis, for giving us freedom of access to the cove at his camping. Reviews by Martin Stokes and an anonymous referee helped us a lot to improve the original manuscript, and are greatly appreciated.

11. References

Ambraseys, N. N. and J. A. Jackson, 1997. Seismicity and strain in the Gulf of Corinth (Greece) since 1694*, J. Earthquake Eng.*, 1, 433-474.

Armijo, R., B.Meyer, G.C.P. King, A. Rigo, D. Papanastassiou, 1996. Quaternary evolution of the Corinth Rift and its implications for the Late Cenozoic evolution of the Aegean. Geophys. J. Int. 126, 11–53.

Avallone, A., Briole, P., Agatza-Balodimou, A.-M., Billiris, H., Charade, O., Mitsakaki, C., Nercessian, A., Papazissi, K., Paradissis, D., Veis, G., 2004. Analysis of eleven years of deformation measured by GPS in the Corinth Rift Laboratory area. C.R. Geoscience 336, 4/5, 301-311, doi:10.1016/j.crte.2003.12.007.

Bard, E., Hamelin, B., Arnold, M., Montaggioni, L., Cabioch, G., Faure, G., Rougerie, F., 1996. Deglacial sea-level record from Tahiti corals and the timing of global meltwater discharge. Nature 382, 241–244.

Bernard, P., Lyon-Caen, H., Briole, P., Deschamps, A., Pitilakis, K., Manakou, M., Boudin, F., Berge, C., Makropoulos, K., Diagourtas, D., Papadimitriou, P., Lemeille, F., Patau, G., Billiris, H., Castarède, H., Charade, O., Nercessian, A., Avallone, A., Zahradnik, J., Sacks, S., Linde, A., 2006. Seismicity, deformation and seismic hazard in the western rift of Corinth: New insights from the Corinth Rift Laboratory (CRL). Tectonophysics 426, 7-30.

Bryan, W. B., Stephens, R. S., 1993. Coastal bench formation at Hanauma Bay, Oahu, Hawaii. Bull. Geol. Soc. Am. 105, 377-386.

Burbank, D. W., Anderson, R. S., 2001. Tectonic Geomorphology, Blackwell science, 274 pp.

Collier, R.E.L. , M.R. Leeder, R.J. Rowe, T.C. Atkinson, 1992. Rates of tectonic uplift in the Corinth and Megara basins, central Greece, Tectonics 11, 1159–1167.

Collina-Girard, J., 1999. Observation en plongee de replats d'erosion eustatique a l'ile d'Elbe (Italie) et a Marie-Galante (Antilles): une sequence bathymetrique modiale? C.R. Acad. Sci. Paris 328, 823-829.

De Martini, P.-M., Pantosti, D., Palyvos, N., Lemeille, F., McNeill, L., Collier, R., 2004. Slip rates of the Aigion and Eliki faults from uplifted marine terraces, Corinth Gulf, Greece. Comptes Rendus Geoscience 336(4-5), 325-334.

Doutsos, T., Poulimenos, G., 1992. Geometry and kinematics of active faults and their seismotectonic significance in the western Corinth-Patras rift (Greece). Journal of Structural Geology 14 (6), 689-699.

Flemming, N.C., Webb, C.O., 1986. Tectonic and eustatic coastal changes during the last 10,000 years derived from Archaeological data, Z. Geomorph. N. F., suppl.-bd. 62, 1-29.

Flotté, N., 2003, Caracterisation structurale et cinematique d'un rift sur detachement: Le rift de Corinthe-Patras, Grece, *These doct.*, 196 pp., Univ. de Paris-Sud.

Fouache, E., Desruelles, S., Pavlopoulos, K., Dalongeville, R., Coquinot, Y., Peulvast, J.-P., Potdevin, J.-L., 2005. Using beachrocks as sea level indicators in the insular group of Mykonos, Delos and Rhenia (Cyclades, Greece), Zeitschrift fur Geomorphologie, suppl. Vol. 137, 37-43.

Gaki-Papanastassiou, K., Papanastassiou, D., Maroukian, H., 1996. Geomorphic and Archaeological - Historical evidence for past earthquakes in Greece. Annali di Geofisica 39 (3), 589-601.

Ge, T., Migeon, W., Szepertyski, B., 2005, L'elevation seculaire des berges antiques et medievales de Bordaux. Etude geoarchaeologique et dendrochronologique, C.R. Geosc., 337, 297-303.

Gómez-Pujol, L., Cruslock, E.M., Fornos, J. J., Swantesson, J.O.H., 2006. Unravelling factors that control shore platforms and cliffs in microtidal coasts: the case of Mallorcan, Catalonian and Swedish coasts. Zeitschrift fur Geomorphologie N.F. Suppl.-Vol. 144, 117-135.

Houghton, S. L., Roberts, G. P., Papanikolaou, I. D., McArthur, J. M., 2003. New ^{234}U-^{230}Th coral dates from the western Gulf of Corinth: implications for extensional tectonics. Geoph. Res. Lett. 30 (19), 2013. doi:10.1029/2003GL018112

Hughen, K.A., Baillie, M.G.L., Bard, E., Bayliss, A., Beck, J.W., Bertrand, C., Blackwell, P.G., Buck, C.E., Burr, G., Cutler, K.B., Damon, P.E., Edwards, R.L., Fairbanks, R.G., Friedrich, M., Guilderson, T.P., Kromer, B., McCormac, F.G., Manning, S., Bronk Ramsey, C., Reimer, P.J., Reimer, R.W., Remmele, S., Southon, J.R., Stuiver, M., Talamo, S., Taylor, F.W., van der Plicht, J., Weyhenmeyer, C.E., 2004, Radiocarbon 46, 1059-1086.

Keller, E., Pinter, N., 1999. Active tectonics – Earthquakes, uplift and landscape, Prentice-Hall, 337 pp.

Kelletat, D., 2005. A Holocene sea-level curve for the eastern Mediterranean from multiple indicators, Zeitchr. Geomorph., suppl. Vol. 137, 1-9.

Kelletat, D. H., 2005b. Notches. In Schwartz, M., (ed.), Encyclopedia of coastal science. Springer, doi 10.1007/1-4020-3880-1_231.

Kennedy, D.M., Dickson, M.E., 2006. Lithological control on the elevation of shore platforms in a microtidal setting. Earth Surface Processes and Landforms 31, 1575-1584. doi : 10.1002/esp.1358

Kershaw, S., Guo, L., 2001. Marine notches in coastal cliffs: indicators of relative sea-level change, Perachora Peninsula, central Greece. Marine Geology 179, 213-228.

Kershaw, S., Guo, L., Braga, J., 2005. A Holocene coral-algal reef at Mavra Litharia, Gulf of Corinth, Greece: structure, history, and applications in relative sea-level change. Marine Geology 215, 171-192. doi:10.1016/j.margeo.2004.12.003

Koukouvelas, I. & Doutsos, T., 1997. The effects of active faults on the generation of landslides in NW Peloponnese. In: Engineering Geology and the Environment , Marinos, G. C., Koukis, G. C., Tsabaos , S. G. C., (Eds), Proc. Int. Symp., A. A. Balkema, Rotterdam, 799-804.

Koukouvelas, I., Doutsos, T., 1996. Implications of structural segmentation during earthquakes: the 1995 Aigio earthquake, Gulf of Corinth, Greece. J. of Struct. Geol. 18 (2), 1381-1388.

Koukouvelas, I., Katsonopoulou, D., Soter, S., Xypolias, P., 2005. Slip rates on the Helike fault, Gulf of Corinth, Greece: new evidence from geoarchaeology. Terra Nova 17, 158-164.

Kontopoulos, N., Zelilidis, A., 1997. Depositional environments of the coarse-grained lower Pleistocene deposits in the Rio-Antirio basin, Greece. In: Engineering Geology and the Environment , Marinos, G. C., Koukis, G. C., Tsabaos , S. G. C., (Eds), Proc. Int. Symp., A. A. Balkema, Rotterdam, 199-204.

Laborel, J., Laborel-Deguen, F., 1994. Biological indicators of relative sea-level variations and co-seismic displacements in the mediterranean region. J. Coast. Res. 10 (2), 395–415.

Laborel, J., Morhange, C., Lafont, R., Le Campion, J., Laborel-Deguen, F., Sartoretto, S., 1994. Biological evidence of sea level rise during the last 4500 years, on the rocky coasts of continental SW France and Corsica. Mar. Geol. 120, 203-223.

Lajoie, K., 1986. Coastal tectonics. In Studies in Geophysics – Active tectonics, National Academy Press, Washington DC, 95-124.

Lambeck, K., Purcell, A., 2005. Sea-level change in the Mediterranean Sea since the LGM: model predictions for tectonically stable areas. Quaternary Science Reviews 24, 1969-1988.

Leeder, M., McNeill, L., Collier, R., Portman, C., Rowe, P., Andfrews, J., 2003. Corinth rift margin uplift: new evidence from Late Quaternary marine shorelines. Geoph. Res. Lett. 30 (12), 1661, doi:10.1029/2003GL017382.

Maroukian, H., Gaki-Papanastassiou, K., Papanastassiou, D. and Palyvos, N., 2000. Geomorphological observations in the coastal zone of the Kyllini Peninsula, western Peloponnesus, Greece and their relation to the seismotectonic regime of the area. Journal of Coastal Research 16 (3), 853-863.

McCalpin, J.P. (ed.), 1996. *Paleoseismology*, Academic press, 588 pp.

McNeill, L.C., Collier, R.E.L., 2004. Uplift and slip rates of the eastern Eliki fault segment, Gulf of Corinth, Greece, inferred from Holocene and Pleistocene terraces. J. Geol. Soc. Lond. 161, 81-92.

McNeill, L., Collier, R., De Martini P.-M., Pantosti, D., D' Addezio, G., 2005. Recent history of the Eastern Eliki fault, Gulf of Corinth: geomorphology, Paleoseismology and impact on palaeoenvironments. Geoph. J. Int.161, 154-166.

Milas, P., 2003. Analysis of tide gauge data (Galaxidi – Aegira tide gauges). NTUA technical report, Department of Topography, Laboratory of Higher Geodesy, 45 pp.

Moretti, I., Sakellariou, D., Lykoussis, V., Micarelli, L., 2003. The Gulf of Corinth: an active half graben? J. of Geodyn. 36, 323-340.

Morhange, C., 2005. Relative sea-level changes in Marseille's ancient harbors (France) during the Late Holocene. Zeitschrift fur Geomorphologie N.F., suppl.vol. 137, 23-28.

Mörner, N.-A., 2005. Sea level changes and crustal movements with special aspects on the eastern Mediterranean. Zeitschrift fur Geomorphologie N.F., suppl.vol. 137, 91-102.

Mouyiaris, N., Papastamatiou, D., Vita-Finzi, C., 1992. The Helice Fault? Terra Nova 4, 124-129.

Palyvos, N., Sorel, D., Lemeille, F., Mancini, M., Pantosti, D., Julia, R., Triantaphylou, M., De Martini, P. M., 2007a. Review and new data on Pleistocene uplift rates at the W termination of the Corinth Rift and the NE Rion graben area (Achaia, NW Peloponnesus). Bulletin of the Geological Society of Greece XXXVII (submitted Oct. 2006, to be published May 2007).

Palyvos, N., Pantosti, D., Stamatopoulos, L., De Martini, P.M., 2007b. Reconnaissance geomorphological observations at the Psathopyrgos and Rion-Patras fault systems (Achaia, NW Peloponnesus). Bulletin of the Geological Society of Greece XXXVII, 12 pp (in press).

Palyvos, N., Pantosti, D., DeMartini, P. M., Lemeille, F., Sorel, D., Pavlopoulos, K, 2005. The Aigion-Neos Erineos normal fault system (Western Corinth Gulf Rift, Greece): Geomorphological signature, recent earthquake history, and evolution. J. of Geoph. Res. 110, B9, B09302, 15 p. doi:10.1029/2004JB003165.

Pantosti, D. & Palyvos, N. (eds), 2007a. 3HAZ Corinth project Deliverable 30 –Maps of active faults, landslides and marine terraces, INGV Roma.

Pantosti, D. & Palyvos, N. (eds), 2007b. 3HAZ Corinth project Deliverable 32 – Dating of paleoearthquakes, INGV Roma.

Papadopoulos, G., Vassilopoulou, A., Plessa, A., 2000. A new catalogue of historical earthquakes in the Corinth Rift, Central Greece: 480 BC – AD 1910, in Papadopoulos, G.A. (ed)., Historical Earthquakes and Tsunamis in the Corinth Rift, Central Greece, Nat. Obs. Ath., Inst. Of Geodynamics, publ. no. 12, 9-120.

Papageorgiou, S., Arnold, M., Laborel, J., Stiros, S., 1993. Seismic uplift of the harbour of ancient Aigeira, Central Greece. Int. J. Naut. Archaeol. 22.3, 275–281.

Pavlides, S., Koukouvelas, I., Kokkalas, S., Stamatopoulos, L., Keramydas, D., Tsodoulos, I., 2004. Late Holocene evolution of the East Eliki Fault, Gulf of Corinth (Central Greece). Quaternary International 115-116, 139-154.

Piper, D.J.W., Kontopoulos, N., Anagnostou, C., Chronis, G., Panagos, A.G., 1990. Modern fan deltas in the western Gulf of Corinth, Greece. Geo-Mar.Lett. 10, 5-12.

Pirazzoli, P.A., Stiros, S.C., Arnold, M., Laborel, J., Laborel-Deguen, F., Papageorgiou, S., 1994. Episodic uplift deduced from Holocene shorelines in the Perachora Peninsula, Corinth area, Greece. Tectonophysics 229, 201– 209.

Pirazzoli, P.A., 1996. Sea-Level Changes – The last 20,000 years. John Wiley & Sons, Chichester, 211 pp.

Pirazzoli, P.A., Mastronuzzi, G., Saliege, J.F., Sanso, P., 1997. Late Holocene emergence in Calabria, Italy. Marine Geology 141, 61-70.

Pirazzoli, P.A., Stiros, S., Arnold, M., Laborel, J., Laborel-Deguen, F., 1999. Late Holocene coseismic vertical displacements and tsunami deposits Near Kynos, Gulf of Euboea, Central Greece. Phys. Chem. Earth (A) 24 (4), 361-367.

Pirazzoli, P.A., Stiros, S.C., Fontunge, M., Arnold, M., 2004. Holocene and Quaternary uplift in the central part of the southern coast of the Corinth Gulf (Greece). Marine Geology 212, 35-44. doi:10.1016/j.margeo.2004.09.006

Pirazzoli, P.A., 2005. Marine erosion features and bioconstructions as indicators of tectonic movements, with special attention to the eastern Mediterranean area. Zeitschrift fur Geomorphologie, suppl. vol. 137, 71-77.

Pirazzoli, P.A., 2005b. A review of possible eustatic, isostatic and tectonic contributions in eight Late Holocene relative sea-level histories from the Mediterranean area. Quaternary Science Reviews 24, 1989-2001.

Poulimenos, G., 1993. Tectonics and sedimentation in the western Corinth Graben, Greece. N. Jb. Geol. Palaont. Mh.10, 607-630.

Poulos, S.E., Collins, M.B., Pattiaratchi, C., Cramp, A., Gull, W., Tsimplis, M., Papatheodorou, G., 1996. Oceanography and sedimentation in the semi-enclosed, deep-water Gulf of Corinth (Greece). Marine Geology 134, 213-235.

Reimer, P.J., McCormac, F.C., 2002. Marine radiocarbon reservoir corrections for the Mediterranean and Aegean Seas. Radiocarbon 44, 159– 166.

Rozos, D., 1991. Engineering geological conditions in Achaia Province – geomechanical characteristics of the Plio-Pleistocene Sediments. PhD Thesis, Department of Geology, University of Patras (in Greek).

Stanley, D.J., Warne, A.G., 1994. Worldwide initiation of Holocene marine deltas by deceleration of sea-level rise. Science, 265, 228-231.

Stefatos, A., Papatheodorou, G., Ferentinos, G., Leeder, M.., Collier, R., 2002. Seismic reflection imaging of active offshore faults in the Gulf of Corinth: their seismotectonic significance. Basin Res. 14, 487-502.

Stewart, I., 1996. Holocene uplift and paleoseismicity on the Eliki Fault, Western Gulf of Corinth, Greece. Annali di Geofisica XXXIX/3, 575-588.

Stewart, I., Vita-Finzi, C., 1996. Coastal uplift on active normal faults: The Eliki fault, Greece. Geoph. Res. Lett. 23 (14), 1853-1856.

Stiros, S.C., Arnold, M., Pirazzoli, P.A., Laborel, J., Laborel, F., Papageorgiou, S., 1992. Historical coseismic uplift on Euboea Island, Greece. Earth Planet. Sci. Lett. 108, 109– 117.

Stiros, S., Pirazzoli, P. A., 1995. Paleoseismic studies in Greece: a review. Quaternary International 25, 57-63.

Stiros, S., Pirazzoli, P., Rothaus, R., Papageorgiou, S., Laborel, J., Arnold, M., 1996. On the Date of Construction of Lechaion, Western Harbor of Ancient Corinth, Greece. Geoarchaeology 11**,** 251– 263.

Stiros, S.C., 1998. Archaeological evidence for unusually rapid Holocene uplift rates in an active normal faulting terrain: Roman harbour of Aigeira, Gulf of Corinth, Greece, Geoarchaeology 13 (7), 731-741.

Stiros, S., Laborel, J., Laborel-Deguen, F., Papageorgiou, S., Evin, J., Pirazzoli, P.A., 2000. Seismic coastal uplift in a region of subsidence: Holocene raised shorelines of Samos Island, Aegean Sea, Greece. Mar. Geol. 170, 41-58.

Stuiver, M., Reimer, P.J., 1993. Extended ^{14}C database and revised CALIB radiocarbon calibration program. Radiocarbon 35, 215-230.

Thornton, L.E., Stephenson, W.J., 2006. Rock strength: a control of shore platform elevation. Journal of coastal research 22(1), 224-231. DOI:10.2112/05A-0017.1

Trenhaile, A. S., 2002. Rocks coasts, with particular emphasis on shore platforms. Geomorphology 48, 7-22.

Trenhaile, A. S., 1987. The geomorphology of rock coasts. Oxford Research Studies in Geography, Clarendon Press, Oxford, 384 pp.

Tselentis, G.-A., Makropoulos, K.C., 1986. Rates of crustal deformation in the Gulf of Corinth as determined from seismicity. Tectonophysics 124, 55-66.

Westaway, R., 2002. The Quaternary evolution of the Gulf of Corinth, central Greece: coupling between surface processes and flow in the lower continental crust. Tectonophysics 348, 269-318.

FIGURE CAPTIONS

Figure 1. Shaded relief and normal fault zones in the Corinth Rift, including previously studied locations with geomorphic evidence of Holocene coastal uplift and the new sites found at the westernmost part of the Rift. Shaded relief map derived from NASA's SRTM DEM. Inset: location of the Corinth Gulf Rift and Geodynamic setting .

Figure 2. Lithological map of the coastal escarpment NW of Lambiri and locations of uplifted Holocene shoreline remains and littoral fauna. The uplifted features are on Holocene littoral conglomerates (mainly), scree and limestone bedrock. The main trace of the Lambiri fault zone is expected to be a short distance offshore, or exactly along the coastline.

Figure 3. Coastal lithologies: a) littoral Holocene conglomerates (in all probability, fan delta foresets), b) limestone with boulder-grade scree and biogenic encustations, c) limestone with cobble-grade scree draping plunging cliff that corresponds to fault plane, and d) limestone and cobble-grade scree with extensive biogenic encrustations. (a, b, c, d): locations 35, 54 (E side), just west of 43 and, between 43 and 50, respectively, in Figure 2.

Figure 4. Surveyed profiles of coastal geomorphological features testifying recent uplift of the Lambiri coastal escarpment. (locations in Figure 2). Values in black rectangles: estimated paleoshoreline elevations (m a.m.s.l.), based on assumptions discussed in the text.

Figure 5. Views of geomorphic evidence of past Holocene sea-level stands in areas I and II (see text for explanations).

Figure 6. Views of geomorphic evidence of past Holocene sea-level stands in area III (see text for explanations).

Figure 7. (a) General view of coastal location 43. (b) The small limestone outcrop at 7.15 m a.m.s.l. where the highest marine fauna (*Lithophaga* sp.) was retrieved from. (c) *Cladocora* sp. corals and thick *Spondylus* sp. in living position (perforated by *Lithophaga* sp.) in an uplifted Holocene bio-herm. Thinner biogenic encrustations are ubiquitous on the conglomerate that constitutes the roof of the cave, as well as all along the stretch of coast from locations 43 to 50.

Figure 8. Views of geomorphic evidence of past Holocene sea-level stands in area V (see text for explanations).

Figure 9. Graphical summary and correlation of the recognised uplifted bench and notch levels. Dashed lines and/or question-marks indicate uncertain features.

Figure 10. (a) Plot of elevations vs calibrated ages of radiocarbon dated *Lithophaga* sp. samples at location 43. Calibrations using with two different marine reservoir corrections are plotted (see text – Triangles: calibration with ΔR -80, Squares: ΔR 380).

(b) "Best fit", most conservative scenario of minimum coastal uplift rate, based on radiocarbon ages of 4 *Lithophaga* sp. samples between 3 and 4.8 m. See text for explanation. Triangles and squares have the same meaning as in (a). For each dated sample, two points are plotted (min and max age, connected by a line). The data points have been «pulled down » at the slowest possible rates that allow them to coincide with the sea-level dataset of Laborel et al. (1994) / Morhange (2005). The datapoints corresponding to the 3 m Lithophaga age have been allowed to be partially an « outlier », to make the minimum uplift rate estimate the most conservative possible. Minimum uplift rates of the order of 1.6 or 1.9 mm/y are obtained (for DR -80 and 380, respectively).

(c) The same graph as in (b) with the data points corresponding to the min/max ages of the two dated *Lithophaga* sp. at 7.1 m fitted to the Guinea sea-level curve of Bard et al. (1996). This fit requires a min uplift rate of 3.7 or 3.0 mm/yr (for DR -80 and 380, respectively). Even higher uplift rates (3.7-4.9 mm/yr) would be necessary to fit the 7.1 Lithophaga to the Tahiti curve or the model of Lambeck & Purcell (2005). See text for explanation.

Figure 11. Various possible interpretations of the shoreline record (see text for explanations). The relative sea-level (RSL) still-stands that the identified narrow benches expectedly correspond to, are portrayed as horizontal bars in the relative sea-level graphs (schematically, implied still-stand timing and durations are arbitrary).

Figure 12. (a) Holocene sea level curves in Mörner (2005, and previous works), from Sweden and other areas. (b) Late Holocene sea-level curve by Laborel et al. (1994), with additional data from Morhange (2005). The curve drawn in magenta in (a) is also plotted in (b) for comparison, to show the differences in the magnitude of Late Holocene sea-level fluctuations between different areas (the two graphs have different horizontal and vertical scales). The green rectangle in (b) indicates the period relevant to the shoreline record discussed herein.

TABLE CAPTIONS

Table 1. Summary of elevations (in metres) of paleoshorelines (between m.s.l. and 3 m a.m.s.l., A to E) in the different areas along the studied stretch of coast, obtained by assigning benches to the lower part of the intertidal zone and notch apices at or close to mean sea-level. The 0.8-0.9 m bench at location 29 (Figure 9) and the 1.5 m elevation for bench B at location 1 are evidently outliers, thus they are not included in the reported synthetic ranges for all

areas and stretch A-A'. Cells in gray color indicate bench levels that are associated with notch remains.

Table 2. Radiocarbon ages for dated samples of marine fauna. Calibrated with the CALIB v. 5.0 software (Stuiver and Reimer, 1993) and marine calibration curve (marine04) by Hughen et al. (2004). Sample locations in **Figure 4**. Measured ages are calibrated with two local correction factors for marine reservoir effect in the Corinth Gulf, following Pirazzoli et al. (2004) (ΔR= -80 and +380 yrs, proposed by Stiros et al., 1992 and Soter, 1998, respectively).

(*) This value is outside the usual range for marine shells (above zero), but does not indicate an erroneous age[1].

(Poz-): Poznan Radiocarbon Laboratory, (BRGM03S206): SEM analysis at BRGM, dating at Beta Analytic.

Table 3. Summary of different minimum estimates for average coastal uplift rate (mm/yr) from different scenarios. The highest uplift rate estimates (in italics), based on the ages of the highest Lithophaga dated (7.1 m), call for verification by further studies (see text for explanations).

[1] The of -9.2 permil may be a result of fractionation during sample preparation process. The d13C values the laboratory determines, albeit fully suitable for correction of ^{14}C ages, they cannot be used for palaeoecological reconstructions. The reason is that they are measured in the graphite prepared from the samples and the graphitisation process introduces significant isotopic fractionation. Furthermore, the AMS spectrometer (unlike normal mass spectrometer) introduces fractionation too. Therefore reported d13C values reflect the original isotopic composition only very roughly. And, the difference between these two exceeds 5 ‰ quite often (T. Goslar, pers. comm. – Poznan Radiocarbon Laboratory)

Figure 1

Click here to download high resolution image

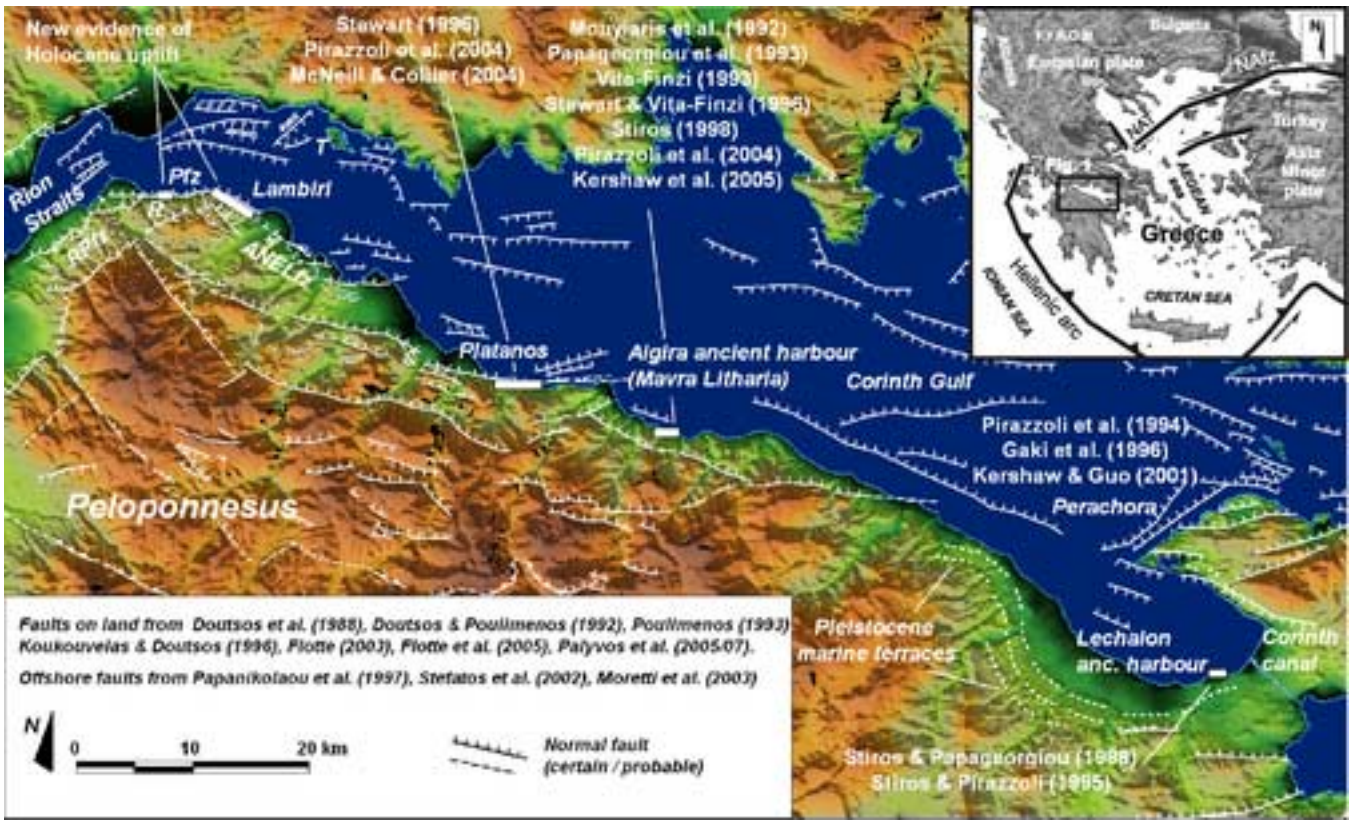

Figure 2

Click here to download high resolution image

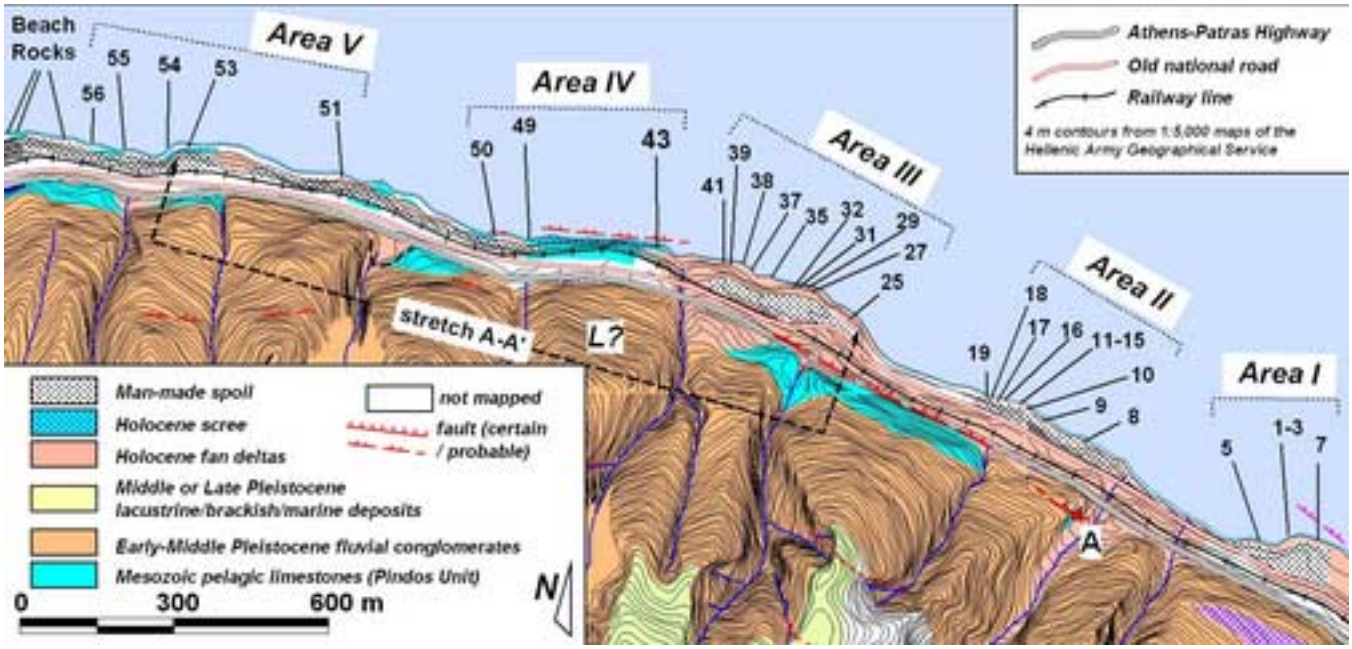

Figure 3

Click here to download high resolution image

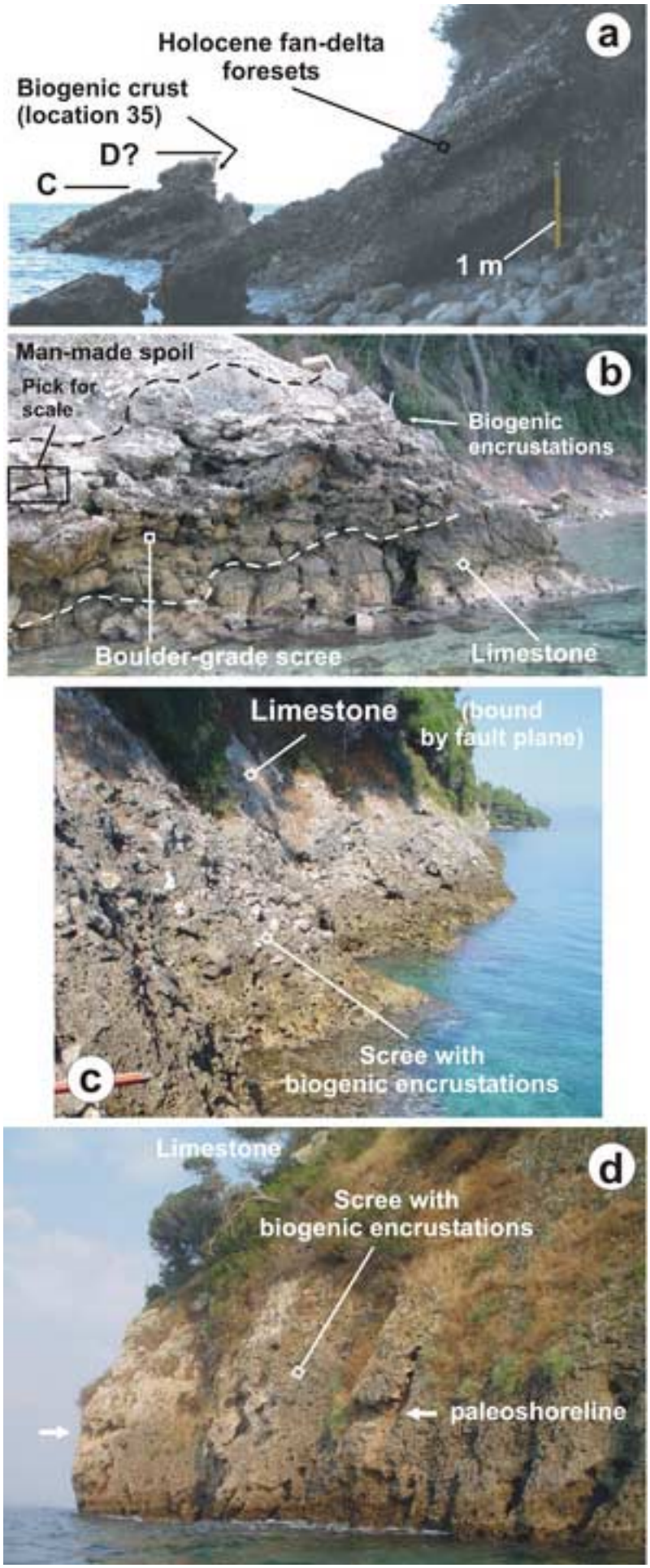

Figure 4

Click here to download high resolution image

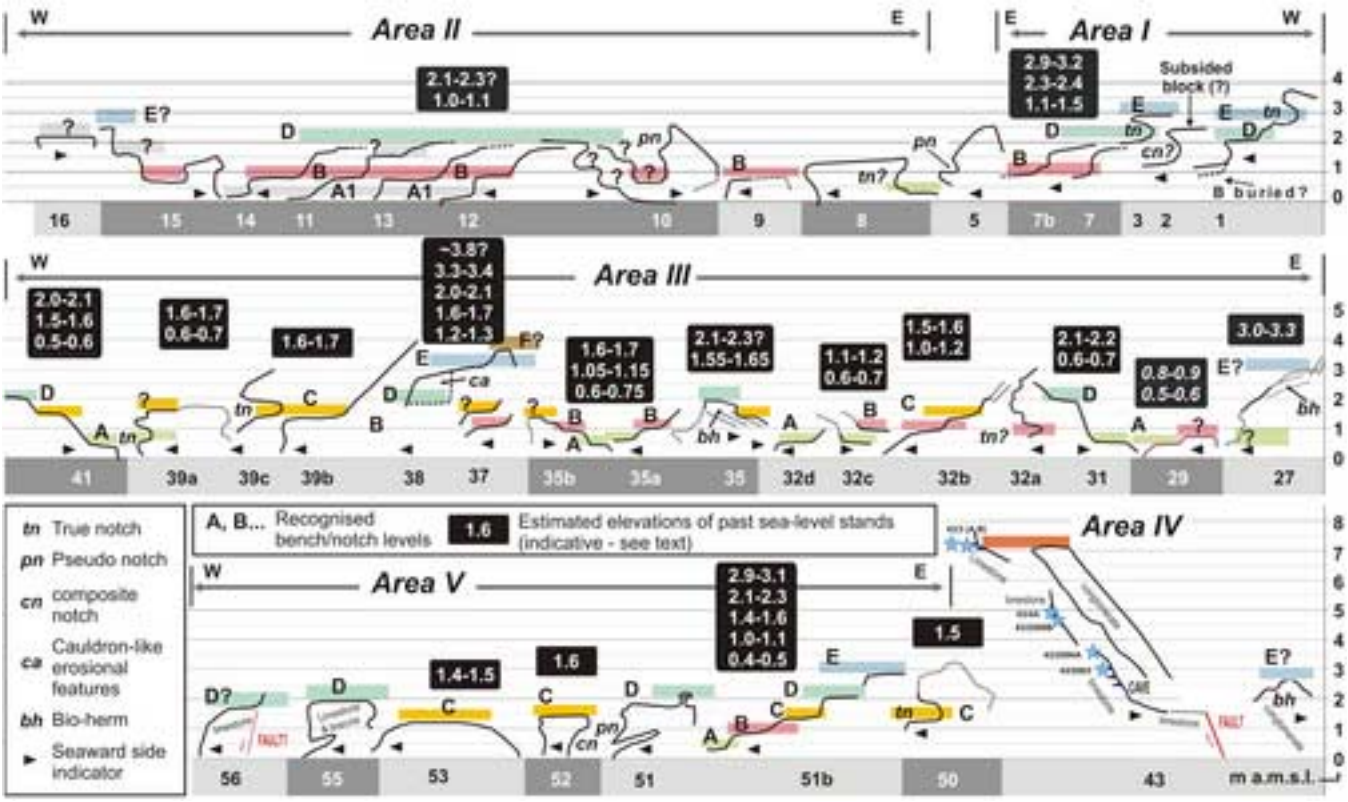

Figure 5

Click here to download high resolution image

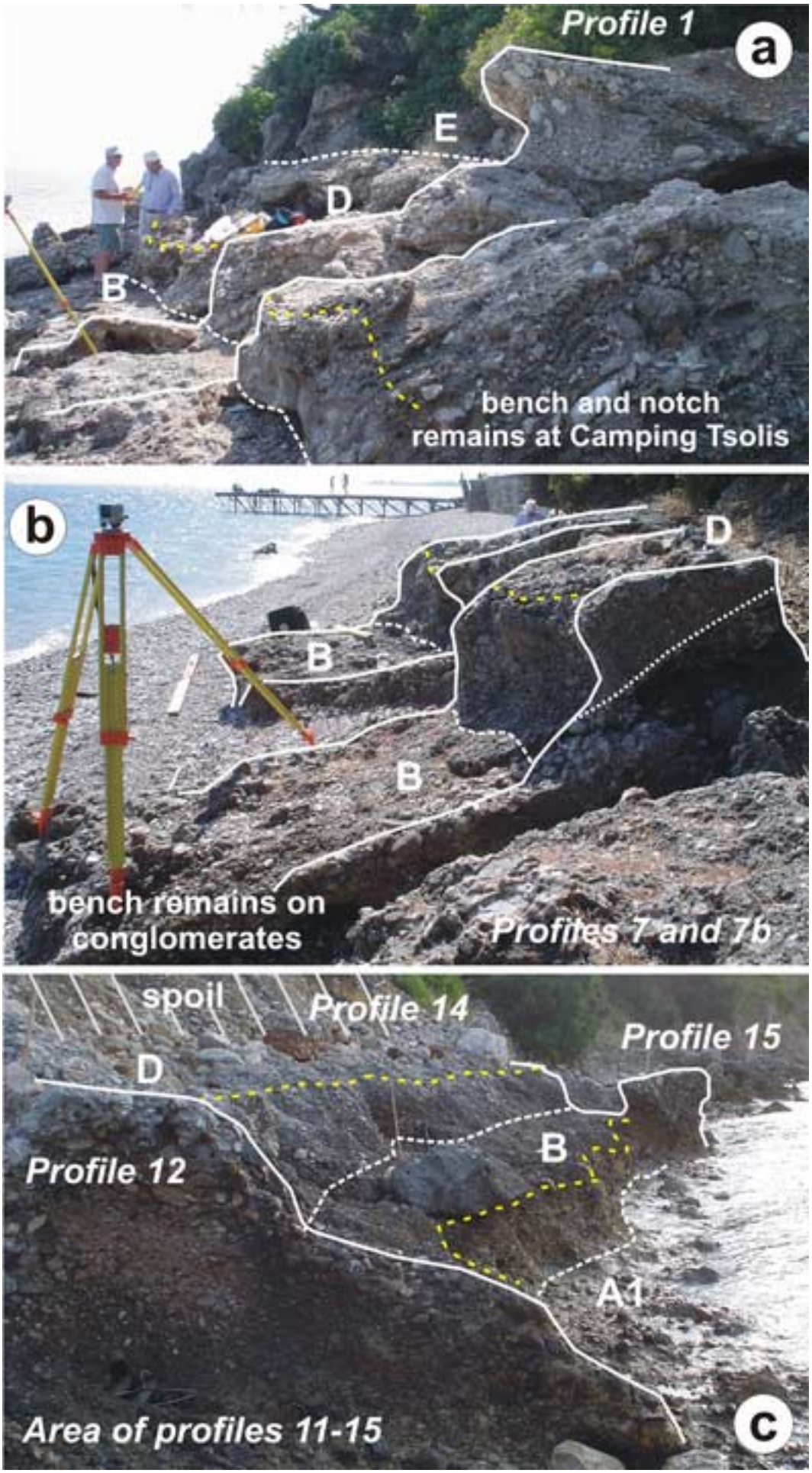

Figure 6

Click here to download high resolution image

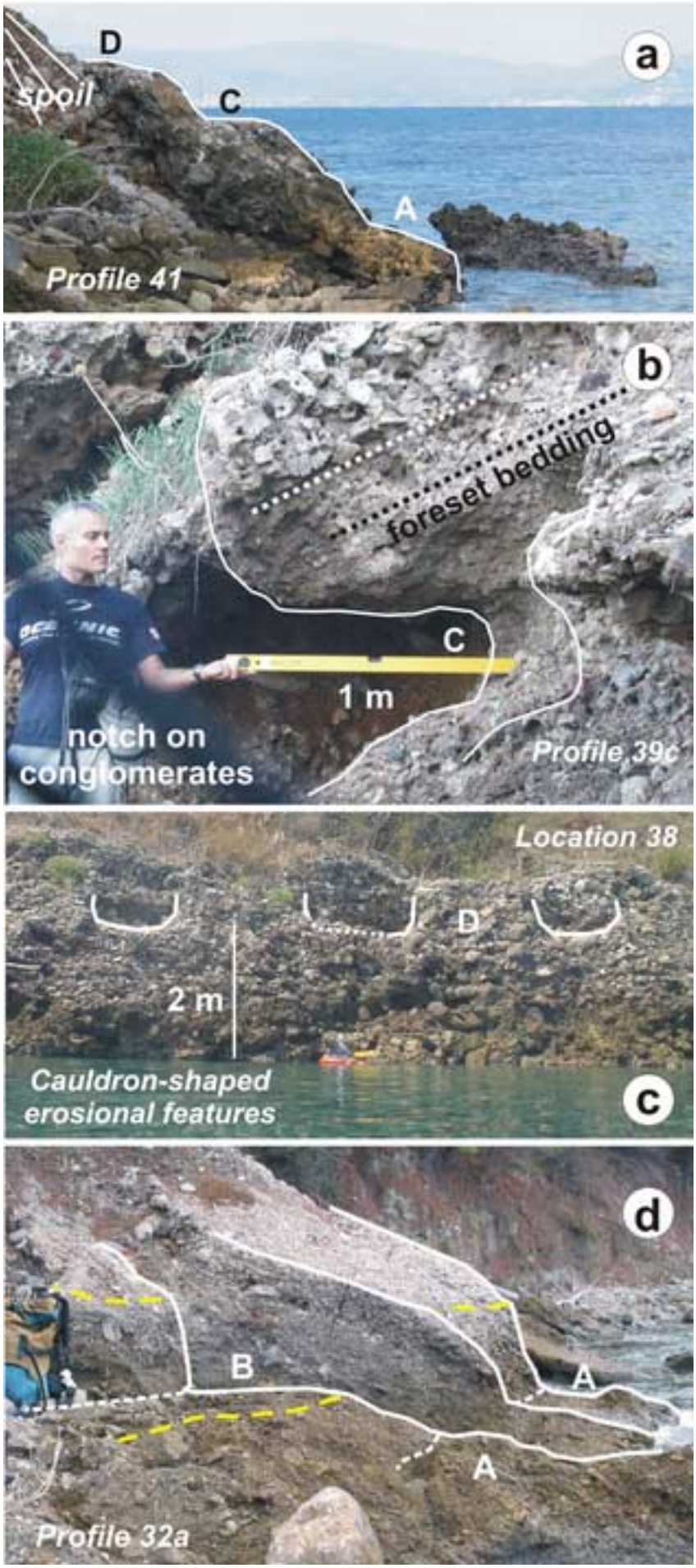

Figure 7

Click here to download high resolution image

Figure 8

Click here to download high resolution image

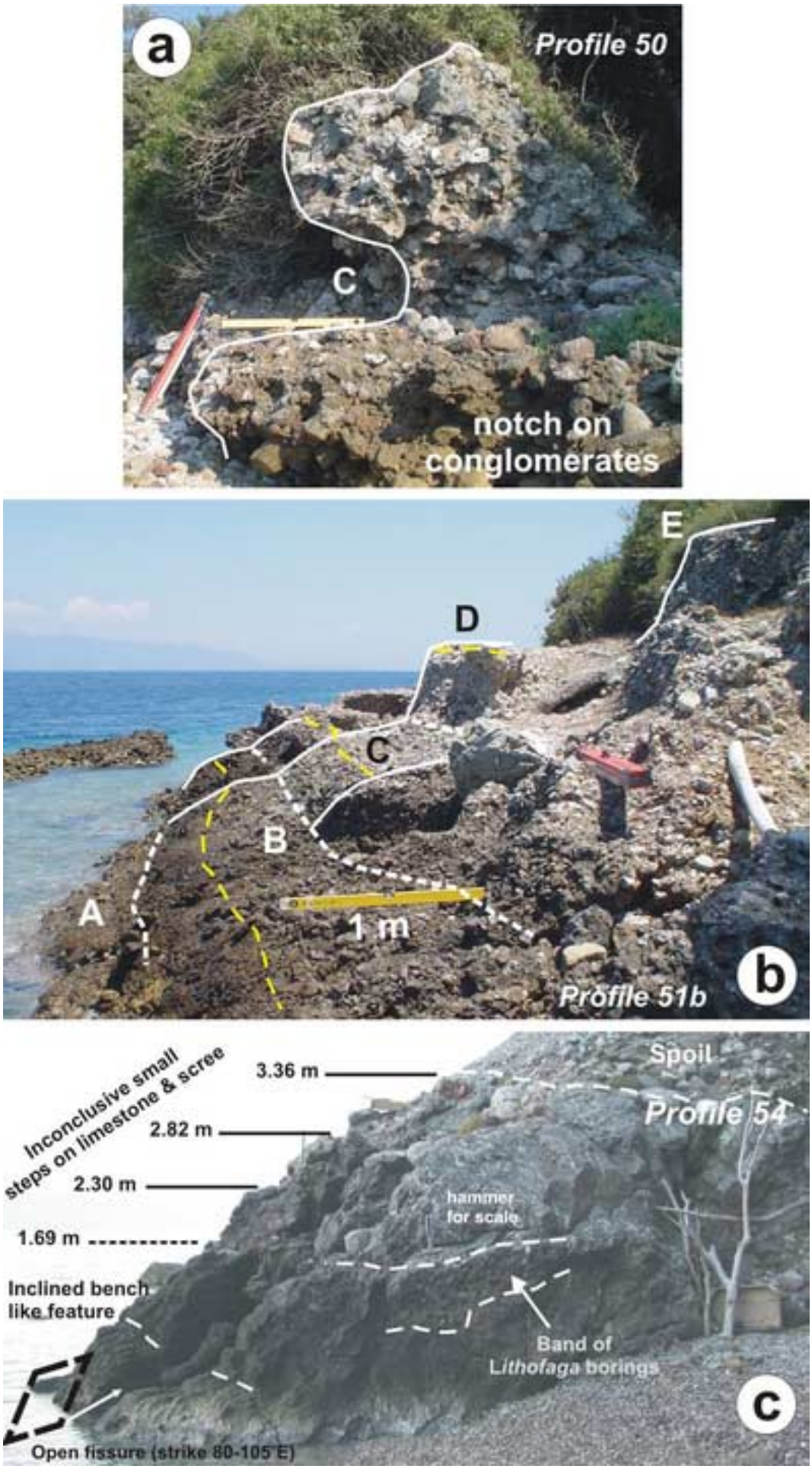

Figure 9

Click here to download high resolution image

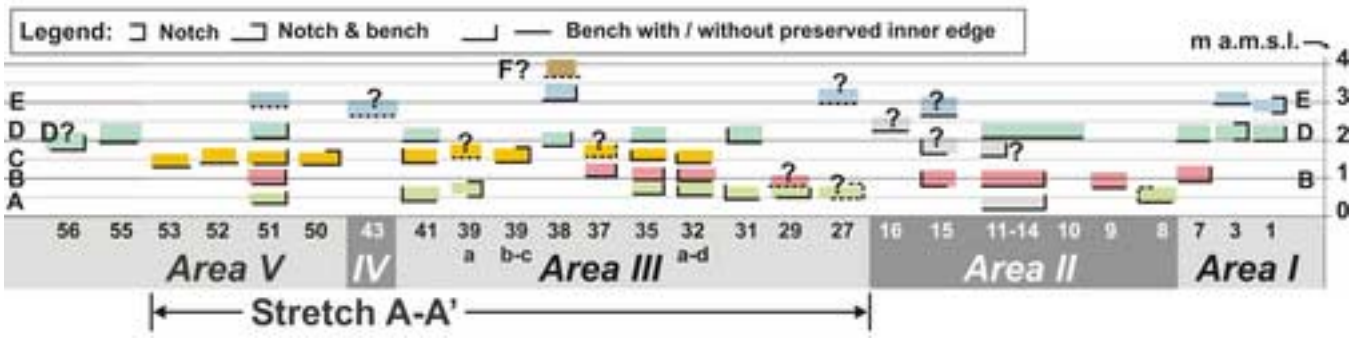

Figure 10

Click here to download high resolution image

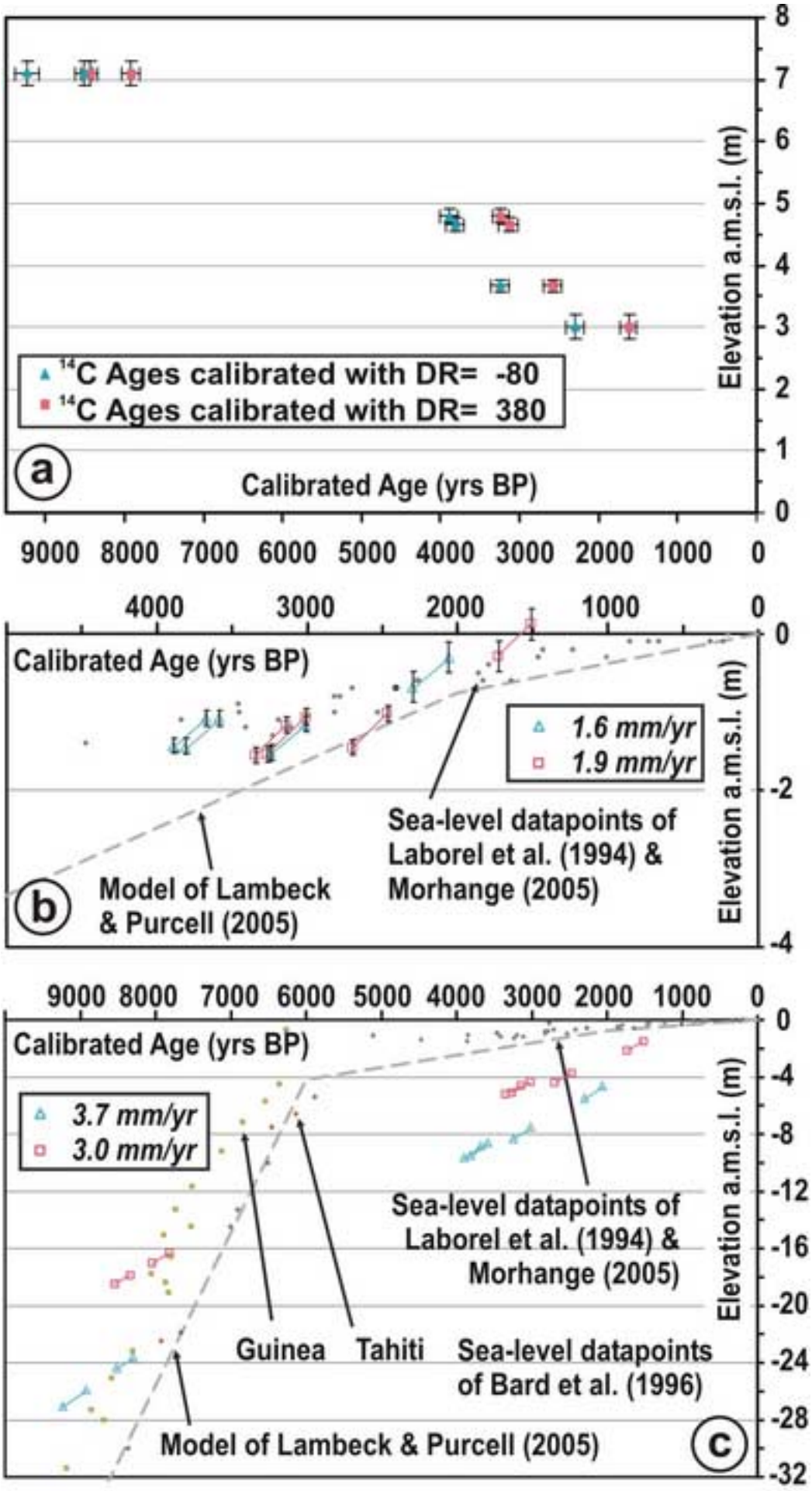

Figure 11

Click here to download high resolution image

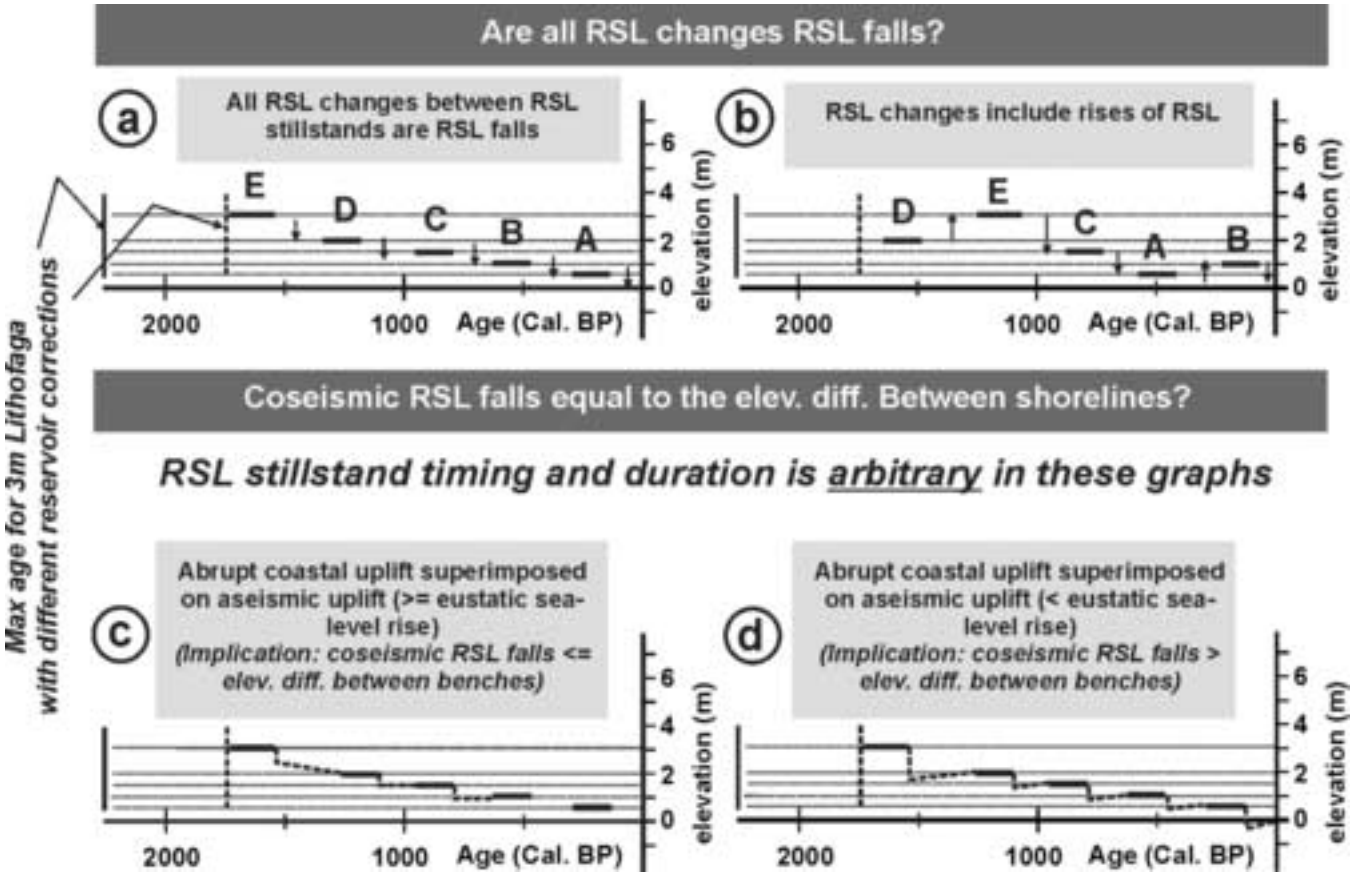

Figure 12

Click here to download high resolution image

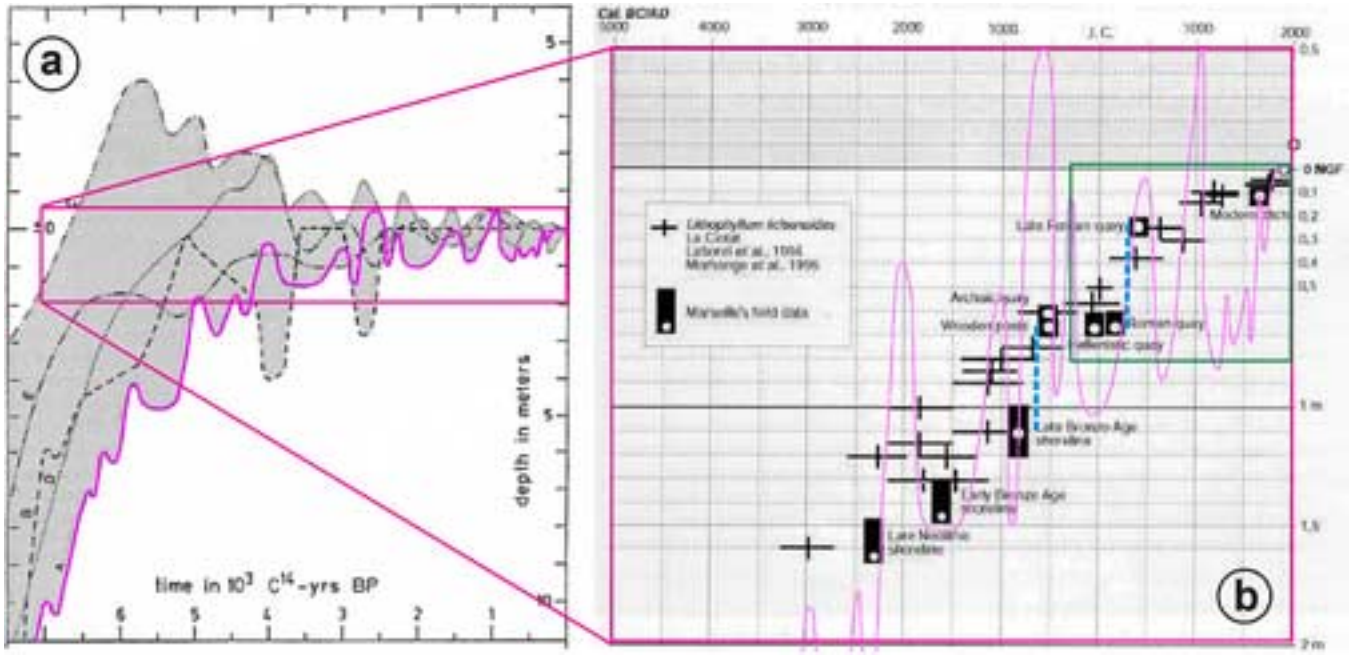

Table 1

	A	B	C	D	E
I		1.1-1.5		2.3-2.4	2.9-3.2
II	0.3-0.5	1.0-1.1		2.1-2.3	2.8-3.0 (?)
III	0.5-0.7	0.8-1.3	1.5-1.7	2.0-2.3	3.0-3.4
IV					2.8-2.9 (?)
V	0.4-0.5	1.0-1.1	1.4-1.6	2.1-2.3	2.9-3.1
ALL	0.3–0.7	1.0-1.3	1.4-1.7	2.0-2.4	2.8-3.4
AA'	**0.4-0.7**	**1.0-1.3**	**1.4-1.7**	**2.0-2.3**	**2.8-3.4**

Table 2

Sample code / Lab. Number	**Elevation a.m.s.l. (m)**	**Material /** Sample type	**$^{13}C/^{12}C$ ratio**	**Conventional R/C age ($^{13}C/^{12}C$ corr.)**	**2 σ calibrated age (cal. yrs BP) ΔR = -80**	**2 σ calibrated age (cal. yrs BP) ΔR =380**
43/3A Poz-15140	*7.1* ± 0.15	*Lithophaga*	4.8 ± 0.5	8350 ± 50	9229-8919	8542-8336
43/3C Poz-15141	*7.1* ± 0.15	*Lithophaga*	2.3 ± 0.3	7850 ± 50	8515-8300	8039-7814
43/4A Poz-15142	*4.8* ± 0.1	*Lithophaga*	-9.7 ± 1.6 (*)	3755 ± 35	3896-3675	3346-3140
43 2006B Poz-17761	*4.66* ± 0.1	*Lithophaga*	2.8 ± 0.3	3680 ± 35	3814-3588	3265-3012
43 2006A Poz-17760	*3.67* ± 0.1	*Lithophaga*	4.7 ± 0.1	3210 ± 30	3244-3015	2699-2468
43/ 2003 BRGM 03S206	*3.0* ± 0.2	*Lithophaga*		2430 ± 40	2298-2061	1728-1512

Table 3

Min AUR from Lithophaga at (m a.m.s.l.)	Laborel et al. (1994) / Morhange (2005)	Lambeck & Purcell (2005)	Bard et al. (1996) [Guinea / Tahiti]
	Delta-R -80		
3.00 m	1.5-1.7	1.75-1.85	
3.66 m	1.5-1.55	1.7-1.75	
4.67 m	~ 1.55	~1.9	
4.80 m	~ 1.52	~1.85	
7.10 m (1)		*~4.4*	*~3.7 [G]* *~4.4 [T]*
7.10 m (2)			*~4.2 [G]* *~4.9 [T]*
	Delta-R +380		
3.00 m	1.9 - 2.15	2.1 - 2.4	
3.66 m	1.6 - 1.75	1.85-1.95	
4.67 m	~1.8	2.0 - 2.1	
4.80 m	~1.8	2.0 - 2.1	
7.10 m (1)		*~4.0*	*~3.0 [G]* *~3.8 [T]*
7.10 m (2)			*~3.7 [G]* *~4.5 [T]*